

CARBON CONCENTRATIONS IN SNYDER CREEK OVER
THE COURSE OF A STORM HYDROGRAPH

By

Corey G. Franklin

A Thesis

Submitted in partial fulfillment
of the requirements for the degree
Master of Environmental Studies
The Evergreen State College

August 2023

©2023 by Corey G. Franklin. All rights reserved.

This Thesis for the Master of Environmental Studies Degree

By

Corey G. Franklin

has been approved for

The Evergreen State College

By

Erin Martin, Ph.D.

Member of Faculty

Date

Abstract

The type of carbon in a stream and its fluctuations can reveal insights into the sources of carbon in a watershed, its mobility, and its potential life cycle. Climate projections for the Pacific Northwest include increased periods of heavy rainfall and total annual precipitation. This makes understanding the effects of storm discharge on carbon fluxes important for estimating the impact climate change will have on carbon cycling for individual ecosystems and globally. This study measured the concentrations of the different fractions of organic carbon and inorganic carbon over the course of four storm hydrographs in a low order stream in the Puget Sound region of Washington between February 28th and April 10th, 2023. Sample analysis showed high average dissolved organic carbon (DOC) concentrations in Snyder Creek compared to those in similar watersheds, but without a clear pattern in its fluctuations. Fine particulate organic carbon (FPOC) concentrations showed major increases at three of the four peak stages of the storm hydrograph. Discharge was negatively correlated with Dissolved Inorganic Carbon (DIC) concentrations and positively correlated with CO₂ outgassing. The DIC was composed mostly of carbonic acid suggesting that it was primarily sourced from biotic respiration as well as some carbonate dissolution. The results from this study do not offer a definitive answer as to how carbon cycling will change with increased precipitation, however, they offer a roadmap for future studies.

Table of Contents

List of Figures.....	vi
List of Tables.....	vii
Acknowledgements.....	viii
Introduction.....	1
Literature Review.....	3
<i>Introduction</i>	3
<i>Terrestrial Sources of River Organic Carbon</i>	4
<i>Soil Organic Carbon</i>	5
<i>Terrestrial Dissolved Organic Carbon</i>	6
<i>Terrestrial Particulate Organic Carbon</i>	7
<i>Autochthonous Sources of River Organic Carbon</i>	10
<i>Inorganic Carbon</i>	12
<i>Storms and Seasons</i>	15
<i>Climate Change Impacts on Stream C Exports</i>	17
<i>Fate of C Downstream</i>	18
<i>Snyder Creek</i>	18
<i>Conclusion</i>	21
Methods.....	22
<i>Site</i>	22
<i>Experimental Design</i>	22
<i>Field Measurements</i>	23
<i>Sampling and Lab Analysis</i>	24
<i>Calculations</i>	27
<i>Statistical Analysis</i>	29
Results.....	30
<i>Discharge</i>	30
<i>Stream Chemistry</i>	32
<i>DOC</i>	34
<i>FPOC</i>	37
<i>CPOC</i>	40

<i>DIC</i>	43
CO₂ Evasion Rates	46
Discussion	47
<i>Discharge</i>	47
<i>DOC</i>	48
<i>FPOC</i>	52
<i>CPOC</i>	53
<i>DIC</i>	55
<i>CO₂ Outgassing</i>	56
Conclusion	58
References	59

List of Figures

Figure 1. Sources of carbon to streams as a function of size and order.....	10
Figure 2. Annual carbon budget of a watershed.....	13
Figure 3. Annual DIC and DOC budget for a temperate headwater stream in Scotland.....	15
Figure 4. Map of the Snyder Creek Watershed.....	19
Figure 5. The Snyder Creek Watershed and the soil types within the watershed.....	20
Figure 6. Box plot of discharge measurements by storm stage.....	31
Figure 7. Graph of stream discharge measurements over the course of the study.....	32
Figure 8. DOC concentrations in Snyder Creek in relation to discharge.....	35
Figure 9. DOC concentrations in Snyder Creek over the course of the sampling stage.....	36
Figure 10. Box plot of DOC measurements by storm stage.....	37
Figure 11. FPOC concentrations in Snyder Creek in relation to discharge.....	38
Figure 12. FPOC concentrations in Snyder Creek over the course of the sampling stage.....	39
Figure 13. Box plot showing the range of FPOC measurements by storm stage.....	40
Figure 14. Box plot showing the range of CPOC measurements by storm stage.....	41
Figure 15. Graph of the relationship between CPOC concentrations and discharge.....	42
Figure 16. Relationship between DIC concentrations and stream discharge.....	44
Figure 17. Graph of the relationship between DIC concentrations in Snyder Creek and pH.....	45
Figure 18. Graph of CO ₂ outgassing rate in Snyder Creek in relation to stream discharge.....	46

List of Tables

Table 1. Stream chemistry and discharge.....	30
Table 2. Stream chemistry and discharge correlation analysis results.....	33
Table 3. Pearson's r values for stream chemistry and discharge correlation.....	34
Table 4. Organic Carbon concentrations.....	34
Table 5. Snyder Creek stream Chemistry and DIC concentrations.....	43
Table 6. Pearson's r values for multiple variable relationship to DIC.....	44

Acknowledgements

I would first and foremost like to thank Erin Martin. I could not have asked for a more supportive, positive, and knowledgeable thesis reader. I would like to give a big thanks to Jenna Nelson for all her help with lab procedures and coordination. Thanks to Mike Ruth for his support and help with the creation of the watershed maps. Thank you to the entire MES faculty for their enthusiasm and support. A big thank you to my cohort particularly those in the soil group: Derek Thedell, Christina Wagner, and Claire Kerwin. Thank you to Annie Goodrich for her constant support and words of praise and encouragement.

I could not have completed this study without the assistance of the UC Davis stable Isotope Facility, Burke Hales team at Oregon State University, and Dongsen Xue at the University of Washington Analytical Service Center.

Introduction

Rivers and streams hold and transport a substantial amount of the global carbon (C) budget, with approximately 5.7 Pg C passing through inland waters each year, three quarters of which evades as CO₂ (Ward et al., 2017; Regenier et al., 2013). The majority of the remaining portion is exported to oceans via stream networks (Ward et al., 2017; Argerich, et al., 2016). The type and amount of C in a stream can give important insight into the mobility of the carbon in a watershed and the likely fate of the carbon in that stream (i.e., is it respired to carbon dioxide or stored as a sink within the watershed) (Neu, 2016; Luce et al., 2014). The concentrations of these pools of C are constantly fluctuating due to water discharge and watershed characteristics such as vegetation, climate, topography, soil type, primary productivity, and river size.

Discharge fluctuation caused by seasonal changes and storm events has the largest control on C fluxes within rivers and streams (Wallin et al., 2010; Medeiros et al., 2012; Voss et al., 2015). Gaining data on the mobility and abundance of C in response to discharge in a stream not only provides crucial insight into the C budget of a watershed but how it can be impacted by changes in climate. This is particularly relevant due to projected climatic changes in the PNW that include more severe drought in the summer and more intense precipitation events during the rest of the year (Voss et al., 2015; Kunkel et al., 2013; Christensen et al, 2007). This will cause drastic changes to stream chemistry and consequently the production and export of carbon (Singh et al., 2021).

The results from studies that have investigated C budgets in small streams suggest that the role of forests as carbon sinks may be far less than is commonly reported because the export of C via streams is not properly accounted for (Argerich et al., 2016; Wallin et al., 2010). Most studies on river C and discharge are on large rivers, but as more data is emerging it has become

clear that headwaters not only play an important role in transporting carbon to larger rivers and eventually the ocean, but also in carbon outgassing to the atmosphere (Marx et al., 2017; Ward et al., 2017; Leithold et al., 2006; Schlessinger & Bernhardt, 2013). As streams transition to higher order rivers the concentration of organic carbon (OC) transitions from allochthonous (terrestrial origins) to autochthonous (aquatic origins) due to changes in riverbank to stream proportion and light availability (Creed et al., 2015). Small streams are responsible for the input of the majority of aged particulate organic matter POM to oceans (Leithold, et al., 2006). Consequently, the watersheds of low order streams are at a high risk of losing relatively stable aged pools of C, (Ward et al., 2017; Leithold et al., 2006). With future storm events projected to increase in the PNW, small streams are at risk of exporting larger than usual amounts of C (Tank et al., 2017; Voss et al., 2017; Medeiros et al., 2012).

In this study the different pools of dissolved and particulate carbon in Snyder Creek, a small coastal stream, were measured during four storm events over the course of a winter season. Samples were collected three times, starting at the beginning of a storm, and ending as the hydrograph receded. The primary objective of this study was to gain a picture of how rapid increases in discharge from winter storms affect the export of the dissolved and particulate C. These findings in turn are meant to provide insight into a future C budget based on climate projections and set a baseline for future studies on similar streams. Similar studies on small low order streams are limited and mostly examine alpine streams which have steep topography, less vegetation, and abundant minerals in the soil. There are very few publicly available studies on streams in this region, in low elevation suburban watersheds, that flow directly into the ocean. This thesis aims to contribute to the knowledge base on the effect that discharge has on organic and inorganic carbon in a small urban stream in the Pacific Northwest.

Literature Review

Introduction

Each year roughly 5.1 Pg of C enters a river or stream where it is either exported to the atmosphere as CO₂, transported to the ocean, or stored in inland waters (Drake et al., 2017; Tranvik et al., 2018; Tank et al., 2018; La Quiere et al., 2016). For reference around 3 Pg of C per year are sequestered by the terrestrial environment. Estimates of the global inland water carbon budget are consistently updated and increased; however, it is likely that around 80% of the C entering watersheds globally is returned to the atmosphere (Drake et al., 2017; Raymond et al., 2013; Cole, et al., 2007). The carbon in rivers is present in both organic and inorganic forms and derived from many different sources and processes. The levels and distributions of these forms of C are constantly fluctuating due to water discharge levels and watershed characteristics such as vegetation, climate, topography, vegetation, soil type, and river size. Discharge fluctuation caused by seasonal changes and storm events have the largest influence over C concentrations within an individual stream (Wallin et al., 2010; Medeiros et al., 2012; Voss et al., 2015). Currently, the consequences of future hydrological extremes on carbon fluxes in streams and rivers remains unclear (Ulseth et al., 2018). Gaining an in-depth knowledge of how they will affect the export and storage of C in all stream types is paramount to understanding the true extent of climate change's impacts and how to prepare for and/or prevent them (Ulseth et al., 2018).

This literature review is an overview of riverine carbon and the variables that control its concentrations. First, the different forms of terrestrial sources of organic carbon and the factors that contribute to their mobilization and input are summarized. Next, autochthonous riverine C and instream primary production is overviewed. Inorganic C and its environmental controls are

touched on next. This section leads to the effects of discharge caused by storm events on stream C and projections of the future climate. The review will end with a more in-depth look at the characteristics of small streams and Snyder Creek.

Terrestrial Sources of River Organic Carbon

Gaining an understanding of the source of carbon and the current form it is in when it enters a stream can reveal its likely fate. Carbon is found in rivers as both organic and inorganic constituents (Ward et al., 2017). Organic carbon can be differentiated based on size into two categories: particulate organic carbon (POC) and dissolved organic carbon (DOC). Coarse particulate organic carbon (CPOC) includes particulates greater than 63 μm and fine POC (FPOC) includes 0.7-63 μm , whereas any carbon smaller than this is categorized as DOC (Ward et al., 2017).

The bulk of carbon in most streams comes from terrestrial sources (Ward et al., 2017). Terrestrial organic carbon also known as allochthonous, is derived from a mix of materials including C₃ and C₄ vascular plant detritus (biogenic), soils, and carbonate and sedimentary rocks (petrogenic) (Ward et al., 2017; Bianchi, 2011). Before ever reaching soil, raindrops collect dissolved organic matter and particulate matter from atmospheric particles and vapor, and then from vegetation (Ward et al., 2017; Neu et al., 2016). When a rain drop reaches soil, it will either permeate the soil or flow overland. This is determined by soil saturation levels which are dependent on soil permeability, vegetation, and slope (Schlesinger & Bernhardt, 2013). The composition and amount of OC transported to a stream depends on vegetation abundance and properties, surface/ soil type and texture, landscape and the time elapsed since previous soil saturation (Neu, 2016).

The size and location of rivers is also important in determining the type of OC they transport (Ward et al., 2017). Small rivers and streams are significant sources of POC containing soil fractions and plant derived fractions especially during storms. As the ratio of river edge to river body decreases, the ratio of dissolved to particulate OC acquired typically increases with the size of a river (Webster et al., 1999).

Soil Organic Carbon

The largest active pool of OC in the world is soil organic carbon (SOC) and contains predominantly DOC and biogenic POC (Bianchi, 2011; Davidson & Janssens, 2006). Temperature, moisture, substrate, and vegetation availability are the primary controls of SOC accumulation and stability in forests (Tank et al., 2018). High average moisture levels and cool average temperatures typically result in the highest rate of SOC accumulation. Soil C concentrations vary greatly within a region as a result of soil substrate, topography, and vegetation. The mean residence time of OC increases by depth, with the oldest pool existing in the soil mineral horizon (~10,000 years) (Bianchi, 2011; Schöning et al., 2006). The lower levels of soil gain relative stability due to chemical and physical processes such as sorption and occlusion as well as natural recalcitrance of certain OM such as lignin (Strawn, 2021, Bianchi, 2011). A 2014 analysis of 281 studies showed mineral soils to have less SOC than organic soil (Camino- Serrano et al., 2014). However, high clay content as well as the presence of Iron (Fe) and Aluminum (Al) oxides can reduce mineralization, allowing for DOC retention due to the high adsorption capacity of clay (Camino-Serrano et al., 2014; Nelson et al., 1990).

Lignin is an organic polymer found almost exclusively in terrestrial vascular plants and constitutes a significant percentage of total plant carbon including up to one third of all living wood. It provides plants structure and is more resistant to degradation by microbes in

comparison to other plant matter such as cellulose, especially in small lower temperature streams (Bianchi, 2011; Jex et al., 2014; Ward et al., 2013). During base stream flows the input of OC and nutrient concentration in a stream originates from these deep soil pools, which result in the input of predominantly older lignin and OC adsorbed to minerals (Strawn et al., 2021, Bianchi et al., 2011). Its abundance and relative resistance make lignin an important key to understanding C cycling in rivers (Ward et al., 2012).

Terrestrial Dissolved Organic Carbon

In most soil the highest concentrations of labile DOC are found on the surface and in the uppermost 20 cm of soil (Neu et al., 2016). High concentrations can also be found at depth in the anoxic conditions of wetlands (Hinton et al., 1998). In order for these pools of DOC to be transported to a stream there must be enough moisture to connect the soils or wetlands to it. A lack of connection allows for a buildup of DOC particularly in shallow soils (Kaplan & Newbold, 2000). Consequently, DOC often sees a major spike in exports that peaks quickly after initial storm / snowmelt surges which typically occur between December and May (Giesbrecht et al., 2020; Neu et al., 2016; Voss et al., 2015). The spike in DOC then quickly recedes before the maximum discharge is reached which results from the labile pools of surface DOC being exhausted and unable to regenerate during periods of high precipitation (Neu et al., 2016, Voss et al., 2015). A model for the mobilization of DOM from heavy rainfall or snowmelt in headwaters is known as the Pulse Shunt Concept (PSC) (Raymond et al., 2016). PSC proposes that headwater streams during storms input a major, underreported portion of the DOC that remains unmetabolized in larger streams and is transported to the oceans. The percentage of DOC that is not metabolized is correlated with the magnitude of the storm (Raymond et al., 2016).

Throughfall, unlike overland flow allows water to move through different soil horizons and gather DOC in ground water before laterally entering rivers and streams (Ward et al., 2017). DOC typically decreases by depth as a result of mineralization, transformation into POC, and inability to be transported vertically. However, due to the many factors that affect its concentration, researchers have had difficulty finding a correlation between DOC by depth and land type (Kaplan & Newbold, 2000). DOC in ground water enters streams through the hyporheic zone. The amount of DOC held in the Hyporheic Zone is controlled in great part by the ratio of DOC in the ground water to the DOC in the stream (Kaplan & Newbold, 2000; Jones et al., 1995). If for example, the hyporheic zone has a higher DOC concentration than the stream it will become a source of DOC. If the inverse occurs, it will become a sink (Kaplan & Newbold, 2000). This is the general rule for the metabolism of the hyporheic zone, but stream and substrate characteristics can bend these rules.

Terrestrial Particulate Organic Carbon

POC concentrations in streams generally increase with precipitation, however the fluxes are more gradual than those in DOC (Tank et al., 2017; Galy et al., 2015; Smith et al., 2013). The majority of POC enters streams during high discharge events, including both terrestrially sourced petrogenic and biogenic particulates (Tank et al., 2017). Therefore, predictions of increased extreme precipitation events caused by climate change will likely increase POC fluxes in streams (Hilton et al., 2012; Galy et al., 2015). However, unlike DOC, pools cannot be quickly depleted suggesting that a changing climate could result in a substantial, sustained increase in POC exports (Galy et al., 2015).

Net primary productivity in the watershed, soil formation rates, tectonic uplift rates, bedrock geology, and topography have a strong control over the type and amount of POC

exported by a stream (Hatten et al., 2012). The quantity of POC transported to rivers is controlled by precipitation which acts as the primary connection between terrestrial POC and bodies of water (Smith et al., 2013). Most studies on POC have been on small steep mountainous river systems with high sediment yields. These studies reveal fossil POC (fPOC) from ancient geological sources to be the primary source of riverine POC. The few studies that have gathered samples from headwaters located in other regions have shown biogenic non-fossil POC (nfPOC) to be the predominant export of POC (Hatten et al., 2012). As a result, storm driven POC makes up a substantial portion of POC in larger bodies of water downstream (Medeiros, 2012; Leithold et al., 2006). Only the burial of modern non-fossil carbon contributes to the global CO₂ sink, as fossil POC is in a recalcitrant form prior to entering the aquatic environment where it is at risk to be respired (Ward et al., 2017; Blair & Aller, 2012). Consequently, having an in-depth understanding of the factors that control the mobilization of fPOC vs nfPOC is of great importance.

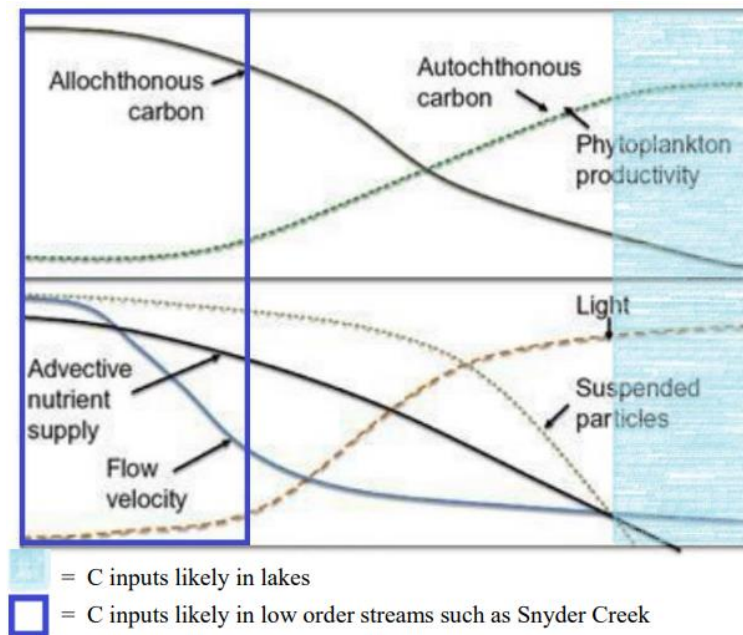
Inputs of petrogenic fossil POC often come from unweathered, exposed sediment that is mobilized by mechanical and chemical weathering in high discharge events and transported to streams (Poesen et al., 2003; Leithold, et al., 2006; Hedges et al., 1992; Ward et al., 2017; Galy et al., 2015). Consequently, mountainous headwater streams located in regions formed by rapid tectonic processes are typically the predominant source of POC and particularly of ancient fractions (Voss et al., 2015). The quantity of fossil POC (fPOC) available for rapid transport during precipitation events directly corresponds to the level of bedrock erosion. In other areas, larger influxes of old fPOC are typically a result of land use changes (Butman et al., 2015). In relatively undisturbed headwaters that are not located in rocky mountainous regions, low concentrations of fossil POC are often present at base-flow (Smith et al., 2013). In most streams,

low total suspended load levels tend to result in a higher proportion of fossil POC concentrations (Smith et al., 2013). However, during high discharge events this pool decreases and is overrun with non-fossil biogenic POC. Although unlikely to be present in Snyder Creek, fossil POC is of particular concern because it is C that was in a recalcitrant form and is now available to be respired in an aquatic environment (Ward et al., 2017).

In a study in the headwaters of a small river in coastal Oregon, POC was primarily derived from contemporary-aged vegetation and soils (Hatten et al., 2012). During high discharge, vegetation derived POC saw around three times the increase compared to petrogenic POC. The POC transported each year by this river is 0.4% of the soil carbon stored in its river basin (Hatten et al., 2012). These findings differ from studies on streams with predominately fPOC exports. A 2001 study on POC export in the Santa Clara River showed that fPOC concentrations plateaued at high flows and declined slightly at peak flow due to supply limitations (Masiello & Druffel, 2001). Studies on other fPOC dominant streams show similar results, which highlight the mobility of plant dominant POC and its abundance in vegetation rich organic soils (Cui, et al., 2016; Hatten et al., 2012).

Figure 1

Sources of carbon to streams as a function of size and order



Adapted from (Schlessinger & Bernhardt et al., 2013)

Autochthonous Sources of River Organic Carbon

Primary production of benthic algae, aquatic macrophytes, and plants are the predominant sources of autochthonous organic carbon (Malone et al., 2022). Light and nutrient availability have the greatest influence over gross primary production (GPP) in streams (Porcal et al., 2015). Nutrient uptake, however, is highly dependent on light so without it little to no primary production will occur regardless of nutrient availability especially in small streams. A 2010 study of a spring fed stream system in south Florida showed that light availability almost perfectly predicted GPP and nitrate uptake (Heffernan & Cohen, 2010). In addition to light nutrient uptake efficiency in streams can decrease from elevated concentrations (Covino et al., 2010, Mulholland et al., 2002). Due to the dependence on light for GPP, autochthonous C rapidly

declines during storm events resulting from murky sediment filled streams (Porcal et al., 2015; Roberts & Mulholland, 2007).

When photosynthesis can occur, nutrient availability is crucial to primary production. For example, streams typically show strong correlation between gross primary production and ecosystem nitrate fluxes. Phosphorous (P) is also important but rarely limiting to primary productivity in streams because it is typically available in river sediments to biota (Schlessinger & Bernhardt, 2013, Francoeur, 2001). In addition to terrestrial availability, flow rate is among the most important influences on nitrogen (N) and phosphorous (P) fluxes in streams. It determines the length of time that water interacts with stream sediment, and it affects the distance before uptake or sorption by N and P occurs (Schlessinger and Bernhardt, Mulholland et al., 2008, Wollheim et al., 2008).

Autochthonous DOM fractions of C within streams see the greatest fluctuations within 24 hours during baseflow (Fasching et al. 2015). This is seen most dramatically during summer months. A 2015 study of an alpine stream measured DOC concentration and photosynthetic active radiation (PAR) for 18 days in August and February (Fasching et al., 2015). The results revealed that the difference between daytime and nighttime PAR measurements was greater in August than February. As a result, autochthonous DOC concentrations in the summer show roughly 2-3 times the in-stream DOC fluctuation over 24 hours compared to the winter. In both months increases in discharge decreased DOC concentration.

Net primary production is typically low in streams and often negative in small streams, due to high rates of respiration in water and low GPP (Hatfield et al., 2019). However, in larger rivers GPP can exceed terrestrial inputs as they diminish, and light availability supports algae and macrophyte growth. Additionally, a major portion of instream GPP is consumed by

invertebrates because algae and macrophytes are preferred to terrestrial OM (Schlessinger & Bernhardt, 2013). In the continental US, aquatic respiration from microbial decomposition accounts for 28% of CO₂ evasion from rivers and streams (Hotchkiss, et al., 2015).

Autochthonous DOC also contributes to total stream exports but makes up a small portion compared to terrestrial DOC.

Inorganic Carbon

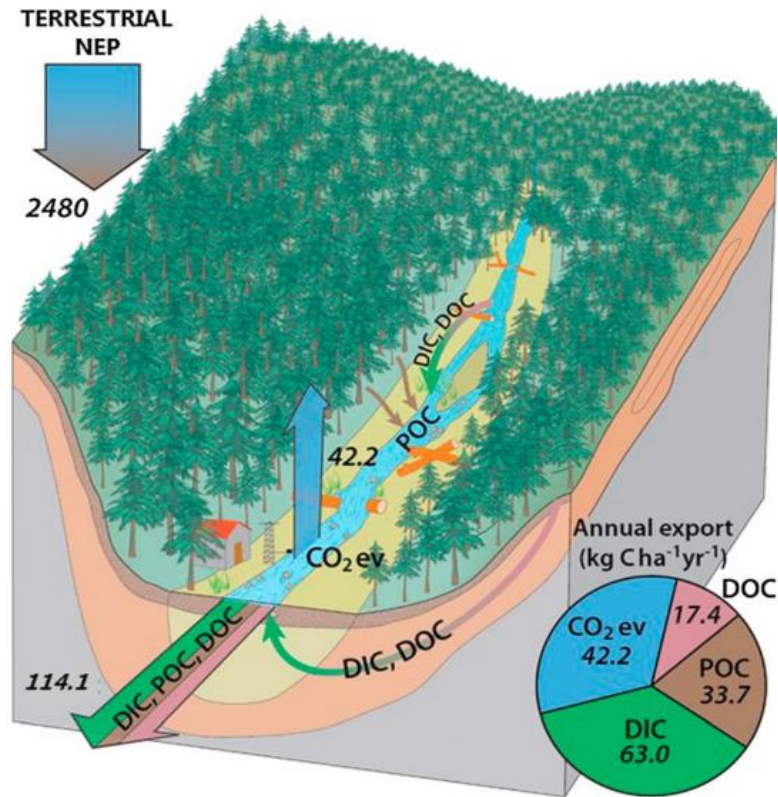
Dissolved inorganic carbon (DIC) in streams includes (carbon dioxide) CO₂, carbonic acid (H₂CO₃), bicarbonate anion (HCO₃⁻), and carbonate (CO₃²⁻). DIC is controlled by groundwater influxes, respiration in the benthic and hyporheic zones of a river, and weathering of carbonate rich rocks (Fellows, et al., 2001; Cole & Prairie, 2009). Temperature can also affect DIC concentrations because CO₂ solubility is inversely related to it (Stumm & Morgan et al., 1996). The constituents that make up DIC have a strong control over pH in small streams (Wallin et al., 2010). Bicarbonate and carbonate concentration is the primary neutralizing force against acidity in water (Cole & Prairie, 2009). Counteractively, dissolved CO₂ is the main acid in most freshwater, making pH a reliable determinant of the balance of these different types of DIC (Cole & Prairie, 2009).

DIC leaves streams laterally to larger rivers, lakes, and oceans and as CO₂ through evasion at the surface. Studies have revealed that almost all fresh water is supersaturated with CO₂ relative to the atmosphere (Aufdenkampe, et al., 2011; Argerich et al., 2016). A 2016 meta study showed global stream CO₂ levels to be between 18 to 738 percent greater than the atmosphere and the hyporheic zone to be 775 to 3,650 times greater (Argerich, 2016). This causes a consistent evasion of CO₂ from rivers to the atmosphere. A 2016 study of the carbon budget of a watershed

in western Oregon revealed that 27% of the annual C exported is evaded as CO₂ (Argerich et al, 2016).

Figure 2

Annual carbon budget of a watershed



HJ Andrews Experimental Forest in western Oregon. Figure from Argerich et al., 2016

The total amount of CO₂ that is emitted by a stream is in part controlled by its size and connectivity to watersheds via soil saturation (Hotchkiss et al., 2015). Low- order streams are often among the most CO₂ saturated bodies of water and consequently contribute significantly more to CO₂ outgassing fluxes than large streams and rivers (Ulseth et al., 2018). The concentration of dissolved CO₂ in comparison to the atmosphere has a strong control over

evasion but not the only one. In Sweden, a 2010 study of 14 headwater stream reaches showed slope to be the most robust predictor of CO₂ evasion (Wallin et al., 2010).

The terrestrial soils surrounding rivers and the rate of mineralization that occurs in them is usually the predominant determinant of CO₂ concentrations in streams (Johnson et al., 2008; Ward et al., 2017). The majority of dissolved CO₂ in headwater streams is sourced from respiration in soil that is laterally transported in groundwater (Johnson et al., 2008; Ward et al., 2017). A 2018 study on multiple first order streams in temperate north-eastern Scotland found that annually 23±11% of terrestrial DOC in streams was respired within an hour of transit time (Demars et al., 2018). Instream respiration of OC on average makes up only 14% of CO₂ production in the smallest streams compared to 39% in the largest rivers (Hotchkiss et al., 2015; Tranvick et al., 2018). Carbonate and bicarbonate enter streams predominantly via the weathering of rocks and minerals driven by dissolved CO₂ and moving water (Cole & Prairie, 2009).

The evasion of CO₂ from streams to the atmosphere is the greatest during high discharge from storm events and snow melt (Wallin et al., 2010). Hydrological pulses from storms generally increase DIC inputs from soil into the stream but depending on its availability will deliver even more terrestrial DOC (Demars et al., 2019; Raymond et al., 2016). This mass influx of DOC can flip the proportion of terrestrial CO₂ to CO₂ from in-stream respiration (Hotchkiss et al., 2015; Demars et al., 2019). The large spike in CO₂ emissions generally mirrors the trend in discharge. There is often a greater correlation between discharge and CO₂ in the most acidic and CO₂ rich streams. (Wallin, et al., 2010). In some small streams heightened CO₂ emissions will remain after storm flow declines due to a high retention capacity of labile DOC in the hyporheic

zone (Demars et al., 2019). Conversely, some severe storms will lower stream metabolism through the removal of standing biomass and riverbed organic matter.

Figure 3

Annual DIC and DOC budget for a temperate headwater stream in Scotland

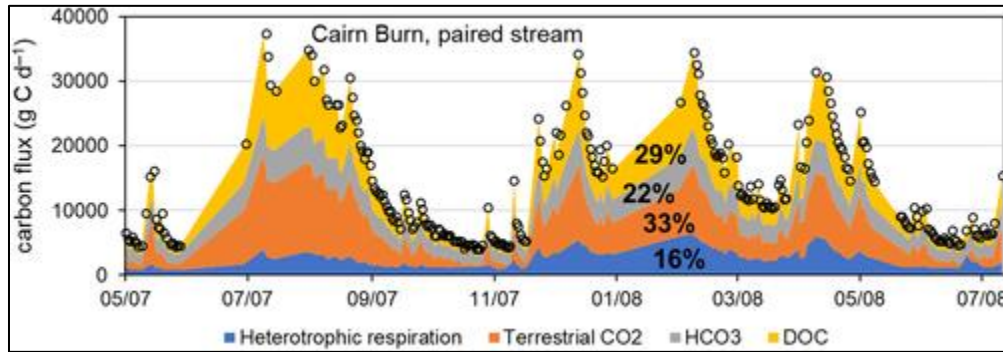


Figure from (Demars, 2018).

Storms and Seasons

Overland flow is not a major source of river C compared to throughfall over the course of a year but is significant during storm events (Ward et al., 2017). The increase in water needs to be significant and sustained enough to mobilize the nutrients. In the Fraser River of British Columbia, increased river discharge causes rapid increases of DOC concentrations from 200 $\mu\text{mol L}^{-1}$ to peak levels of 700-900 $\mu\text{mol L}^{-1}$ over the course of days at the start of spring discharge increase due to snowmelt (Voss et al., 2015). Lignin concentrations then decrease as river flow continues to increase in spring, suggesting that shallow labile DOC has been largely depleted (Ward, 2012). The Fraser River study is an example of a watershed that is snowpack or glacially impacted, which tends to peak right as discharge begins to peak in the spring (Giesbrecht et al., 2022; Voss et al., 2015). Watersheds in mountainous regions with rain driven hydrology experience C export that is spread out over the rainy season as opposed to one or two major spikes (Giesbrecht et al., 2022). Lowland watersheds such as Snyder Creek show even

greater temporal variance in DOC export which will be expanded upon further at the end of the literature review (Giesbrecht et al., 2020).

In a 2001 study in Virginia, Buffam and colleagues found that although a stream only experiences stormflows during 4% of the year, they constitute 36% of the annual discharge and more than 50% of DOC and N inputs (2001). As a result, a fivefold increase of bacterial growth was observed as well as a slight increase of DOM bioavailability, further contributing to the storm caused riverine C (Buffam, et al., 2001).

In addition to the magnitude of discharge change, the precipitation and stream flow the conditions preempting a storm have a noticeable effect on the amount of DOC exported by a stream (Guarch- Ribot & Buttarini, 2016; Neu et al., 2016; Voss et al., 2015). Both periods of extended drought and precipitation preceding an increase in discharge can limit the amount of terrestrial DOC exported by a stream. In addition to being quickly depleted from preceding storms as described previously, drought can reduce the ratio of C in DOM as a result of photobleaching and microbial degradation of the limited terrestrial OM in the water (Guarch- Ribot & Buttarini, 2016). Photobleaching of DOM was shown to occur even in a heavily forested stream during extended droughts (Guarch-Ribot & Buttarini, 2016). The first storms after extended periods of low precipitation are often characterized by high DOM export in headwaters and relatively low DOC concentrations (Guarch-Ribot & Buttarini, 2016). Increasingly dry summers in the pacific northwest make these findings more applicable to the future C dynamics in western Washington's streams (Guarch- Ribot & Buttarini, 2016, Christensen et al., 2007).

POC pools are at a high risk of export in extreme weather events. Greater periods of soil saturation because of increased precipitation can promote the release of POC (Knorr, 2012). Storm caused landslides and sheetwash events cause massive POC fluxes, increasing the relative

rate of POC to DOC mobilization (Tank et al., 2018). Unlike DOC pools which are quickly depleted, terrestrial POC pools have been historically stable without a little risk of depletion (Blair et al., 2010; Tank et al., 2018). Consequently, as extreme weather events increase a near bottomless supply of POC is available to be exported and potentially re-mineralized (Blair et al., 2010).

Climate Change Impacts on Stream C Exports

In the Pacific Northwest, climate change is projected to cause an increase in extreme weather events as well as increased drought in summers and higher annual temperatures (Kunkel et al., 2013; Christensen et al., 2007). There is expected to be 13% (\pm 7%) more days that experience greater than 1 inch of rain in 2050 in comparison with the beginning of the century (Klos et al., 2014; Kunkel et al., 2013; Christensen et al., 2007). Meanwhile summer rainfall is projected to decrease by 6%-8% although some models predict a far greater degree of drought (Mote et al., 2010; Christensen et al., 2007). Hydrological Models show initial decreases in annual stream flow with a small increase by 2040, however stream flow is projected to increase by 30.3% by the 2080s (Wu et al., 2013). Annual temperatures are projected to steadily increase by 1.68° C during the same time frame and summer temperatures by 2.10° C (Wu et al., 2012). This will result in drastic changes to stream chemistry and consequently the production and export of carbon (Singh et al., 2021). The type and amount of C in a stream and how changes in flow and temperature affect it is dependent on stream and watershed characteristics (vegetation, surface/ soil type and texture, landscape, etc.) (Neu, 2016; Luce et al., 2014). Globally, the input of C into rivers increases annually by 0.01 to 0.02 peta-grams and 3-9% of DOC that enters rivers is aged C caused by anthropogenic disturbance (Reginier et al., 2013; Butman et al., 2015). Increase in temperature and precipitation threaten to remove old soil OC that constitutes a major

portion of the terrestrial carbon sink (Eglinton et al., 2021). As climate change progresses, plant biomarkers indicate that older and relatively stable C deposits are increasing their presence in streams globally (Eglinton et al., 2021).

Fate of C Downstream

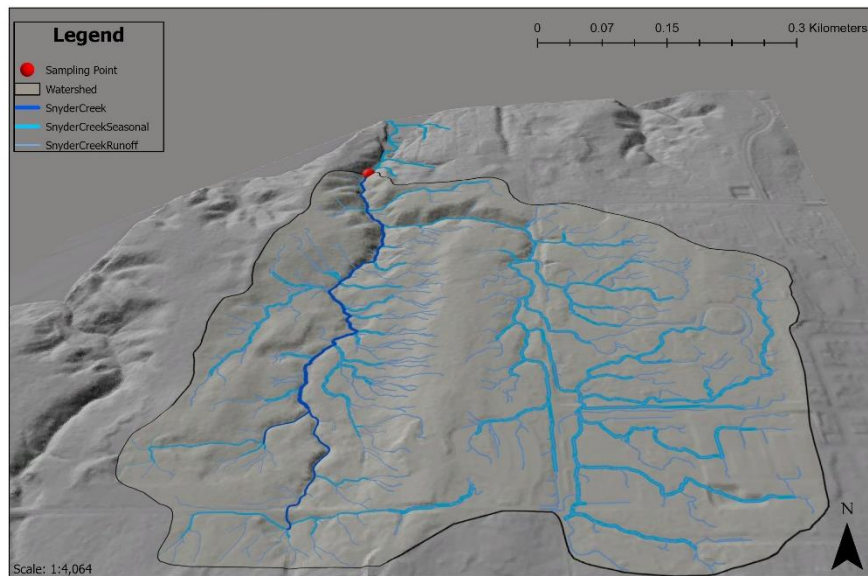
Recent estimates on the fraction of carbon that enters rivers annually, between $\frac{1}{4}$ and $\frac{1}{5}$ of the carbon makes it to the open ocean, with the rest being trapped in coastal sediments, estuaries or returned to the atmosphere (Raymond et al., 2013; Voss et al., 2015; Drake et al., 2017). However, the amount OC that reaches recalcitrant long-term storage in oceans is not well understood (Le Quéré, 2016). It is estimated that coastal sediments make up as much as 90% of the OM buried in the ocean in the last 10,000 years (Burdige, 2005; Ward et al., 2017). Recently, researchers have shown that terrestrially derived DOC is injected into the deep ocean via the global meridional overturning circulation (Medeiros et al., 2016). Small rivers likely contribute a major portion of OM reaching these ancient pools because they are responsible for the input of the majority of aged POC to oceans (Leithold, et al., 2006; Ward et al., 2017). POC sequestered by marine sediments can be stored on a millennial time scale as opposed to DOC which is quickly remineralized soon after reaching the ocean (Hedges et al. 1997). A 2012 study tracked upland sediment and particulate organic carbon biomarkers from a high river discharge and found that OC traveled significantly further down river than during base river flow to the point of saltwater intrusion (Medeiros et al., 2012). The relative recalcitrance of OC exports in low order streams underlines their importance in contributing to long term C storage.

Snyder Creek

In 2022 for a study by Giesbrecht and colleagues categorized the Pacific Northwest by watershed types and measured the DOC seasonality and DOC concentration across all twelve watershed types (Giesbrecht et al., 2022). The study defined watershed types based on variables that control hydro biogeochemistry which include topography, climate, land cover, and geography. The Snyder Creek Watershed is classified as a rain (shadow) lowlands- central watershed (RLC). DOC roughly mirrored runoff over the course of the year, which was similar to many of the other rain dominant watersheds. The peak DOC concentrations were in late fall to early winter with runoff peaking shortly after. Both levels then steadily decreased until the end of summer. Overall, The RLC revealed relatively plentiful DOC stocks with gradual changes in seasonal DOC concentrations and runoff. These findings are in contrast with DOC concentrations in most small headwater streams in high elevation watersheds (Voss et al., 2015; Ulseth et al., 2018).

Figure 4

Map of the Snyder Creek Watershed



Map of the Snyder Creek Watershed, Snyder Creek, the creek’s seasonal high flow tributaries, and runoff paths. The red dot represents the sampling sight for the study. The watershed above the sampling point is surrounded by a bold

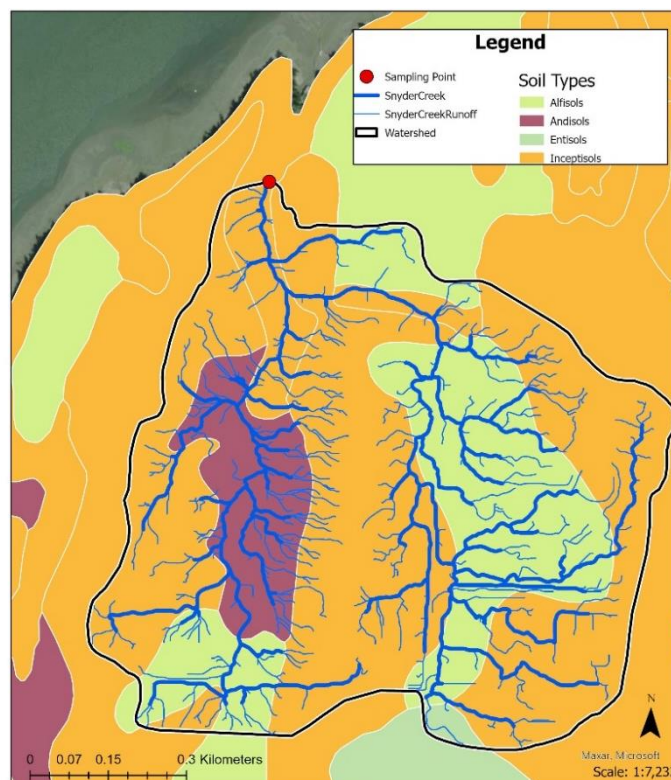
black line, Snyder Creek is represented by a dark blue line, seasonal tributaries are shown as light blue lines, and runoff paths are represented by a thin light blue line. Map was created by Corey Franklin.

Snyder Creek is a perennial first order stream that flows into the Eld Inlet with a stream channel that is 2 ¼ kilometers long (WFC, 2007). The watershed is in a secondary Douglas Fir dominant coniferous forest that receives an average of 127 cm of precipitation per year. The 60-day low flow for the stream is estimated at 1 CFS and the monthly 10% exceedance flow (10% of the year) was 10 CFS as of 1998 (Powers & Saunders, 1998; WDFW, 1994).

Most of the watershed is made up of soil classified as moderately fine to moderately coarse in texture having a moderate rate of infiltration and runoff (USDA). The lower half of the stream bed is made up of fine soil with low rates of infiltration. The soils range between slightly to strongly acidic (USDA).

Figure 5

The Snyder Creek Watershed and the soil types within the watershed



The Inceptisols in the watershed are specifically Alderwood Gravelly Sandy loam (8% to 15% degree slopes), the Entisols are Skipopa Silt loam (3 to 15% degree slopes), the Andisols are Giles silt loam (15-30% slope) and the Alfisols are Xerothents (0 to 5% slope). The soil base map is provided by the USDA Natural Resources Conservation Service. The map was created by Corey Franklin

Conclusion

As discussed in this review, the different fractions of organic and inorganic carbon entering and exiting a stream constantly fluctuate due to a myriad of environmental controls. Currently there has been minimal data collected on the carbon cycling characteristics in small coastal low elevation streams. The studies done on streams most similar to Snyder showed that increasing discharge occurred months earlier than streams with snowmelt driven hydrology and consequently discharge influenced C fluxes occurred earlier as well (Giesbrecht et al., 2022; Argerich et al., 2016; Voss et al., 2017). There was also less variation in DOC and DIC concentration over the course of the year than higher elevation streams (Giesbrecht et al., 2022, Argerich et al., 2016; Voss et al., 2017).

This study looked at the DOC, POC, and DIC concentrations in Snyder Creek in relation to storm discharge over a 40-day period in late winter. This data was used in conjunction with the findings summarized in this literature review to better understand the influence that storm discharge has on Snyder Creek watershed and could have in the future. The Snyder Creek watershed has the soil and topographic characteristics typical of a low elevation headwater stream in this region of the PNW. Making it a suitable proxy for similar water sheds. Determining site-specific variables that influence C cycling can open the door to more accurate C models and informed actions.

Methods

Site

The sampling site selected for this study was chosen near the mouth of Snyder creek, ~200 meters up stream to avoid saltwater intrusion from the ocean. Snyder creek is located in Olympia Washington in a mixed conifer temperate forest. The coordinates for the sampling site are 47°05'05.3"N, 122°58'28.0"W. The sampling sight was located at a straight section of the creek roughly two meters in width at baseflow.

Experimental Design

Sample collection took place during four storms and between each storm at base flow for the period extending from February 28th and ending April 10th. The storms were chosen based on weather reports (weather.gov). The website provided precipitation estimates in six-hour blocks. A storm period was chosen for sampling if there was at least one time block with a projected precipitation estimate of ~0.10 inches or more. The non-storm sampling occurred at least two days after the prior storm on a day with no precipitation. Samples and measurements were taken three times over the course of each storm and once for the non-storm stages. To determine when the measurements and sampling occurred during a storm, the projected storm window (starting with the first hour of projected precipitation and ending with the last) was broken into three evenly spaced time stages. An exception to this rule was that if the greatest precipitation projection did not fall within the middle stage, it could be shifted to encompass it (this did not have to occur). The three stages are defined in this study as the storm rising stage (S1), the height of the storm stage (S2), and the storm falling stage (S3). The sampling times were scheduled to occur in the latter half of each of the three storm stages to allow for the changing precipitation to impact the stream discharge. Due to the inherent inaccuracies of weather forecasts, as well as

logistical difficulties (e.g., transportation, equipment malfunctions, etc.) the sampling times did not always fall perfectly within the planned stage of the storm. However, the sampling times mostly happened within their allotted third of the storm (i.e., storm rising, storm falling). It is also important to note that there is a delay in precipitation falling and discharge reflecting it, meaning that discharge could still be increasing during the last third of the storm.

Field Measurements

The data collected from in field measurements include temperature, depth, water velocity, pH, and dissolved oxygen concentrations. The methodology for sample collection and lab analysis of the samples are described in the next section.

Discharge

Velocity measurements were made in a straight section of the river downstream of where the other measurements were taken. Measurements were collected in accordance with (Hauer & Lamberti, 2007). The width of the water surface at this point in the stream was recorded. Five equally spaced observation points were then determined along the width of the creek and the depth of each point (d_x) was measured using a measuring stick (cm). The mean velocity of each point (v_x) was measured at 60% of the depth of each point using a swoffer meter. Discharge for partial sections of the creek were calculated using the following equation:

$$q_x = v_x \left[\frac{(b_{(x+1)} - b_{(x-1)})}{2} \right] dx \quad (1)$$

In this equation $b_{(x+1)}$ is the distance from the observation point to the next point and $b_{(x-1)}$ is the distance from the observation point to the previous point, q_x therefore is the discharge for one partial section. Total discharge (Q) (m^3/s) was found by adding each partial section together.

Water Chemistry

The following parameters were measured using a YSI PRO 2300 probe: dissolved oxygen concentration in units of milligrams per liter (mg/l) and percent saturation (%), conductivity in micro siemens per centimeter ($\mu\text{S}/\text{cm}$), salinity in parts per thousand (ppt), and temperature ($^{\circ}\text{C}$) of the stream. The barometric pressure was calibrated in the probe using the most recent measurement reported from a known location and adjusted for elevation. The conductivity sensor was calibrated using a 250 ml graduated cylinder filled with 130 ml of freshwater KCl Calibration Standard. After calibrating the probe, the sensor was put into the water and left until the readings became consistent.

The pH of the stream was measured using an Oakton Acorn Series pH meter and pH electrode. The pH was calibrated using pH standards 4,7, and 10 in the field. Five measurements were taken with at least 5 minutes between each measurement and averaged for a final pH.

Sampling and Lab Analysis

Coarse Suspended Sediment (CSS)

CSS samples were collected by filling a 1-liter graduated cylinder by placing it in the stream, then pouring through a $63\ \mu\text{m}$ sieve attached to a funnel, with the filtrate poured into the carboy. This was repeated ten times for approximately 10 L of filtered stream water. The sediment in the sieve was transferred to a bottle using distilled water and labeled with the amount of water that ran through the sieve. The sediment samples were then filtered onto a pre weighed $47\ \text{mm}$ ($0.45\ \mu\text{m}$) cellulose acetate filter on a filter tower, dried overnight at $60\ \text{degrees C}$ in a drying oven, and weighed. The dry weights of the sediment were divided by the volume of water that filtered through the sieve to obtain CSS concentrations. This process was repeated three times for each sample and the resulting concentrations were averaged.

Coarse Particulate Organic Carbon (CPOC)

The PETG bottles used in this step were submerged in a 10% hydrochloric acid (HCl) bath overnight prior to sampling. To gather the CPOC sample, a plankton net (20 μm) was submerged in the stream for 10 minutes. The particles collected in the net were then rinsed into a 125 ml acid washed PETG plastic bottle using distilled water and stored in a freezer post collection. Prior to analysis, the sample was thawed, and most of the water in the bottles was removed using a pre-combusted glass pipette, and the remaining sediment and water was then poured into a glass petri dish. The remaining water was again removed from the petri dish and then the petri dish containing the sediment was dried overnight at 60° C (UC Davis, Stable Isotope Facility, N.D.). The weight of the sediment in all the capsules minus the weight of the capsule(s) were recorded (between 30 mg and 40 mg) and the capsules were sent out for analysis to the University of Washington Analytical Service Center. The analysis was performed using a 2400 CHN analyzer (Perkin Elmer Co.). When the results were received, they were converted from weight % OC to mg/l using the CSS concentrations.

Fine Particulate Organic Carbon (FPOC)

The GF/F filters used for this step were prepared by combusting them in a muffle furnace for five hours at 500°C. The water in the carboys that previously had the CSS removed was poured into a churn splitter. While being agitated, it was transferred into a filter tower with a pre-combusted 47 mm (0.7 μm) GF/F filter (Rosenheim et al., 2012). The filter was labeled with the volume of water filtered, and then dried overnight at 60 degrees C. Ten circular pieces were punched from the filter and folded into a tin capsule and sent out for analysis to University of California Davis Stable Isotope Facility. When the results were received from the lab they were adjusted based on the percentage of the GF/F filter that was sent out for analysis. This number

was then divided by the volume of water filtered through the GF/F filter to obtain the FPOC concentration.

Dissolved Organic Carbon (DOC)

The glass bottles used for this step were combusted in a muffle furnace for five hours at 500°C. The water from the carboy that passed through the GF/F filters was used for DOC analysis. The sample was collected from the bottom chamber of the filter tower after the last round of filtration to avoid contamination from previous samples. The water was then poured into a pre-combusted 40 ml glass bottle and labeled with the volume of water that passed through the filter. The sample was stored in a freezer prior to being sent out for analysis to the University of Washington Analytical Service Center. The analysis was performed using a TOC/TN analyzer.

Fine suspend Sediments (FSS)

Between 100 ml and 2.5 L of stream water was run through pre-weighed 47 mm (0.45 µm) cellulose acetate filters. The filters were labeled with the amount of water and left to dry overnight in a drying oven at 60°C and reweighed. The dry weights of the sediment were divided by the volume of water that filtered through the sieve to obtain FSS concentrations. This process was repeated three times for each sample and the resulting concentrations were averaged. This process was repeated three times for each sample and the resulting concentrations were averaged.

Dissolved Inorganic Carbon (DIC)

DIC samples were collected by partially submerging the opening of a glass beer bottle in the stream, so as to minimize bubbling. The bottles were cleaned with soap and water prior to sample collection. One drop of mercuric chloride was then added to the bottles containing ~315

ml of water using an eyedropper (Hales et al., 2004). The bottles were then sealed with a cap crimper in the field and sent out for analysis to Oregon State University. The analysis was performed using a Burke-o-lator TCO₂ analyzer (Hales et al., 2004). The returned data included total DIC and Alkalinity which was used to calculate DIC species abundance and gas evasion rates for Snyder Creek.

Calculations

DIC Species Calculations

The acid dissociation constants (K₁, K₂) for the different samples were calculated using the in-stream temperatures (Guarch- Ribot and Buttarini, 2012). The coefficients used were dependent upon temperature and pressure and were determined from Stumm and Morgan (1996). The following quadratic equation was then used:

$$(CA)[H^+]^2 + K_1(CA - DIC)[H^+] + K_1K_2(.CA - 2DIC) = 0, \quad (2)$$

to solve for H⁺ (Hydrogen ion) (Follows et al., 2006). Next, the inorganic carbon species (bicarbonate (HCO₃), carbonic acid (H₂CO₃), carbonate (CO₃)) were solved by inserting H⁺, DIC (dissolved inorganic carbon), CA (alkalinity), and the acid dissociation constants into the following equations (Garch-Ribot and Buttarini, 2012):

$$CA = 2[CO_3] + [HCO_3] + [OH] - [H] \quad (2)$$

$$DIC = [H_2CO_3] + [HCO_3] + [CO_3] \quad (3)$$

$$K_1 = \frac{[H] * [HCO_3]}{[H_2CO_3]} \quad (4)$$

$$K_2 = \frac{[\text{CO}_3] * [\text{H}]}{[\text{HCO}_3]} \quad (5)$$

$$K_w = [\text{OH}][\text{H}]. \quad (6)$$

CO₂ Outgassing Rate Calculations- Henry's law coefficient (K_H) was then solved for the samples by plugging in their temperatures in kelvin into the following equation (Weiss, 1974; Wanninkhof, 1992):

$$K_H = e^{(-58.0931 + 90.5069(100/T) + 22.294 \ln(T/100))}. \quad (7)$$

The partial pressure of CO₂ in the water ($p\text{CO}_{2w}$) was determined using the equation:

$$K_H = [\text{H}_2\text{CO}_3] / p\text{CO}_2. \quad (8)$$

The atmospheric $p\text{CO}_2$ levels were found using data from the NOAA's Pacific Marine Environmental Laboratory carbon program that was collected from Nannos Orca buoy in Dabob bay, which was the program's closest location to Snyder Creek. However, the buoy is still ~40 miles from the sampling site and is only an approximation of the $p\text{CO}_{2atm}$ levels at the site. The water velocity measurements (w) obtained in field were then used as a proxy to determine the gas transfer coefficient (K_{600}) using the equation (Alin et al., 2010):

$$K_{600} = 13.82 + 0.35w. \quad (9)$$

Finally, the following equation was used to find the outgassing rate in Snyder Creek (Weiss, 1974):

$$F = k_{600} * K_H (p\text{CO}_{2w} - p\text{CO}_{2atm}). \quad (10)$$

Statistical Analysis

A Shapiro-Wilk's test for normality was used to determine if the variables were normally distributed. If the data was not normally distributed the data was logarithmically transformed prior to the use of statistical tests that assume normality (Pearson's correlation, Analysis of Variance (ANOVA) and retested for normality. If the data was normally distributed an ANOVA was used to assess if the different organic C pools varied depending on the stage of the storm event and between events during non-storm stages. A post hoc Tukey- Kramer analysis was then performed to determine which storm stages had significantly different values. If the data was not normally distributed the Kruskal-Wallis test was used instead.

A Pearson's correlation coefficient test was used to assess the correlation between the different carbon pools and discharge. The test was also used to examine the correlation between carbon pools and sample order (over the course of the seasonal hydrograph). Additional uses of Pearson R analyses include stream chemistry data and C concentration correlations, inorganic and organic carbon correlations, and chemistry data and discharge correlations. If the data was not normally distributed a Spearman's rank correlation was used instead.

Results

Discharge

Discharge was measured during each of the 15 sampling events. The discharge of the stream during sampling stages (Table 3) ranged from 0.14 m³/s to 0.64 m³/s with a mean of 0.29 m³/s and a standard deviation of 0.14 m³/s. The mean and median discharge that occurred during the projected height of the storm was greater than the other stages. The rising and falling periods had average discharges that were also greater than during the non-storm discharges. Discharge measurements were statistically different between types of storm stages ($F_{3,11} = 4.867$, $p = 0.022$). In particular, discharge measurements taken during the stages at the height of the storms (S2) were significantly higher than measurements taken during rising storm stages (S1) and non-storm measurements (NS) (Table 1).

Table 1

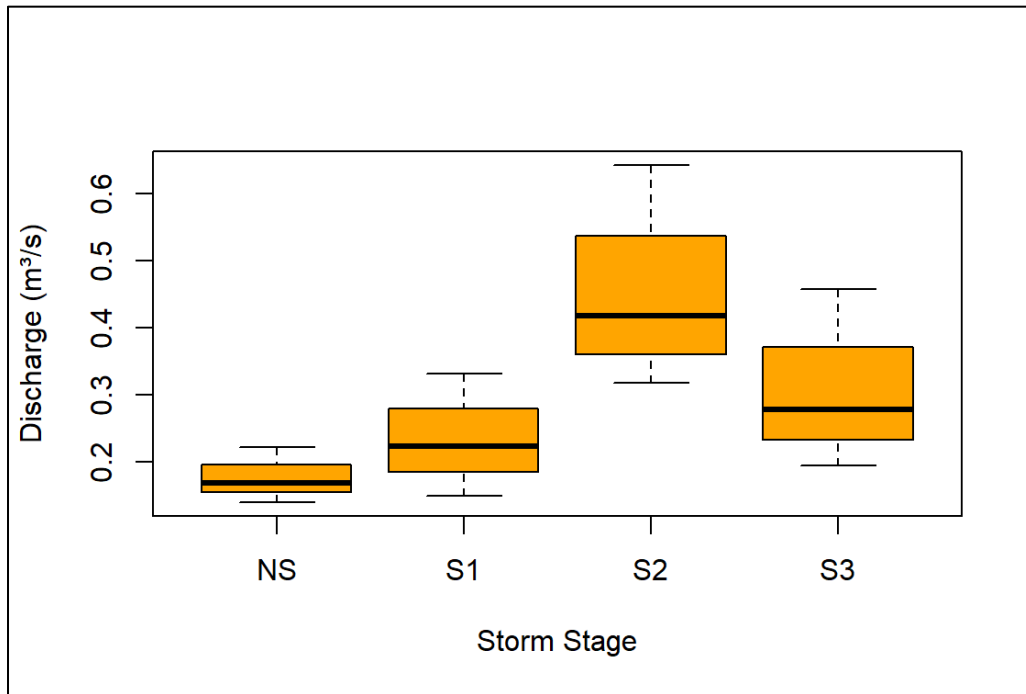
Stream Chemistry and Discharge

	Non-Storm (NS)	Rising Storm Stage (S1)	Peak Storm Stage (S2)
Rising Storm Stage (S1)	0.894	N/A	N/A
Peak Storm Stage (S2)	0.023	0.050	N/A
Falling Storm Stage (S3)	0.418	0.769	0.234

This table shows the p-values of a post hoc Tukey- Kramer test on an ANOVA comparing discharge measurements by storm stage. The table is organized so that the two storm types (X & Y axis) corresponding to a cell to the p-value of that comparison. Orange highlights signifies statistically significant p-values.

Figure 6

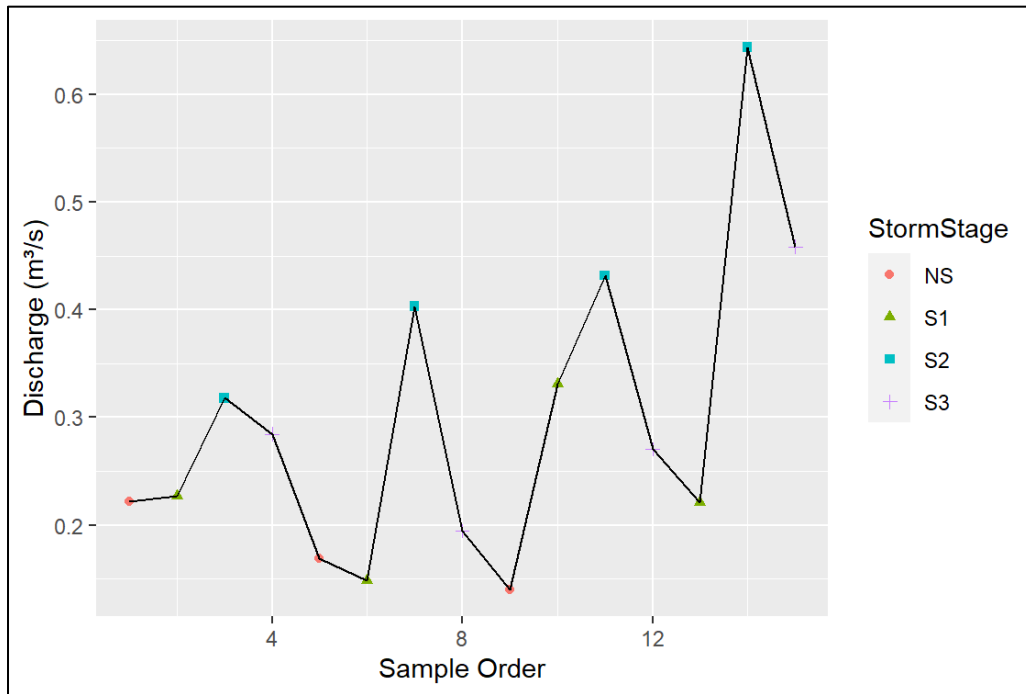
Box plot of discharge measurements by storm stage



For each box the bold line represents the median value, the outer edges of the boxes represent the 1st and 3rd quartiles of the data, and the whiskers show the minimum and maximum.

Figure 7

Graph of stream discharge measurements over the course of the study



The graph shows the stream discharge measurements over the course of the study from February 28th to April 10th. The colored symbols represent the stage of the storm that each measurement was taken during.

A moderate positive correlation coefficient suggests that discharge increased over the course of the study ($r=0.52$, $p=0.047$). The discharge at the height of the storms increased from storm to storm and had a 102% increase from the first measurement on March 8th to the last measurement of April 9th. These findings suggest that overall discharge may have been increasing over the course of the study, which would have been a result of storm flow, and not non-storm flow.

Stream Chemistry

The measurements included under the title of stream chemistry are pH, temperature, salinity, conductivity (spc), and dissolved oxygen. The mean pH was 7.32, the standard deviation (σ) was 0.11, and the pH ranged from 7.17 to 7.45. However, three pH values are missing due to

equipment malfunctions and therefore statistical analysis that includes pH will not reflect all samples. The mean dissolved oxygen levels were 11.07 mg/l, had a σ of 0.55 mg/l, and ranged from 10.31 mg/l to 11.96 mg/l. The mean in stream temperature was 9.47°C, had a σ of 0.74°C, and ranged from 8.4°C to 11.01°C. All salinity levels were either 0 or 0.1 ppt.

Table 2

Stream chemistry measurement and discharge (Q)

Sample #	Date	Storm Period	Temp (C°)	pH	DO (mg/L)	SPC (μ S/cm)	Sal (ppt)
1	28-Feb	NS	8.4	7.44	11.94	150.3	0.1
2	12-Mar	S1	8.4	7.41	11.96	145.5	0.1
3	12-Mar	S2	8.8	7.21	11.68	101.0	0.0
4	13-Mar	S3	8.7	N/A	11.79	111.9	0.1
5	22-Mar	NS	9.9	7.35	10.88	154.7	0.1
6	31-Mar	S1	9.5	7.45	10.35	157.9	0.1
7	31-Mar	S2	9.3	7.17	10.40	100.0	0.1
8	1-Apr	S3	9.2	7.31	10.76	124.8	0.1
9	5-Apr	NS	8.9	7.44	10.31	149.1	0.1
10	6-Apr	S1	9.1	7.24	10.80	95.3	0.0
11	6-Apr	S2	10.0	7.27	11.07	106.9	0.1
12	7-Apr	S3	10.0	7.34	11.05	14.1	0.1
13	8-Apr	S1	10.0	N/A	11.05	136.9	0.1
14	9-Apr	S2	11.1	N/A	10.88	69.9	0.0
15	10-Apr	S3	9.8	7.18	11.07	105.9	0.1

Stream chemistry measurements and discharge (Q) from in stream measurement over the course of the sampling stage.

A Pearson's correlation was used to analyze the relationship between discharge and stream chemistry measurements. In relation to discharge, pH was negatively correlated with discharge ($r=-0.85$, $p= 0.0005$). Temperature was positively correlated with discharge ($r=0.57$, $p= 0.027$). SPC was moderately, negatively correlated with discharge ($r=-0.571$, $p=0.026$). Dissolved oxygen and Salinity did not have statistically significant results.

Table 3

Pearson's correlation test results for the relationship between Stream Chemistry values and discharge

	SPC ($\mu\text{s/cm}$)	Salinity (ppt)	Temp ($^{\circ}\text{C}$)	DO (mg/L)	pH
Pearsons r	-.571	-.499	.569	-.013	-.848

Orange highlights signifies statistically significant p-values with moderate to strong r values.

Table 4

DOC and POC concentrations and discharge (Q)

Sample #	Date	Storm Period	Q (m^3/s)	DOC (mg/L)	CPOC (mg/L)	FPOC (mg/L)
1	28-Feb	NS	0.222	20.6	0.44	0.00*
2	12-Mar	S1	0.227	20.8	0.03	0.08
3	12-Mar	S2	0.318	12.3	0.69	0.13
4	13-Mar	S3	0.285	7.1	0.31	0.51
5	22-Mar	NS	0.169	14.6	0.05	0.23
6	31-Mar	S1	0.149	15.0	0.64	0.15
7	31-Mar	S2	0.403	10.4	1.12	3.21
8	1-Apr	S3	0.195	17.9	1.46	0.97
9	5-Apr	NS	0.140	9.7	0.16	0.23
10	6-Apr	S1	0.331	15.0	0.11	1.18
11	6-Apr	S2	0.432	9.2	0.27	0.11
12	7-Apr	S3	0.271	12.7	0.12	0.43
13	8-Apr	S1	0.221	9.2	0.72	0.32
14	9-Apr	S2	0.643	10.0	0.08	2.92
15	10-Apr	S3	0.458	9.7	1.22	0.70

Dissolved and Particulate organic carbon concentrations and discharge (Q) from in stream measurement over the course of the sampling stage.

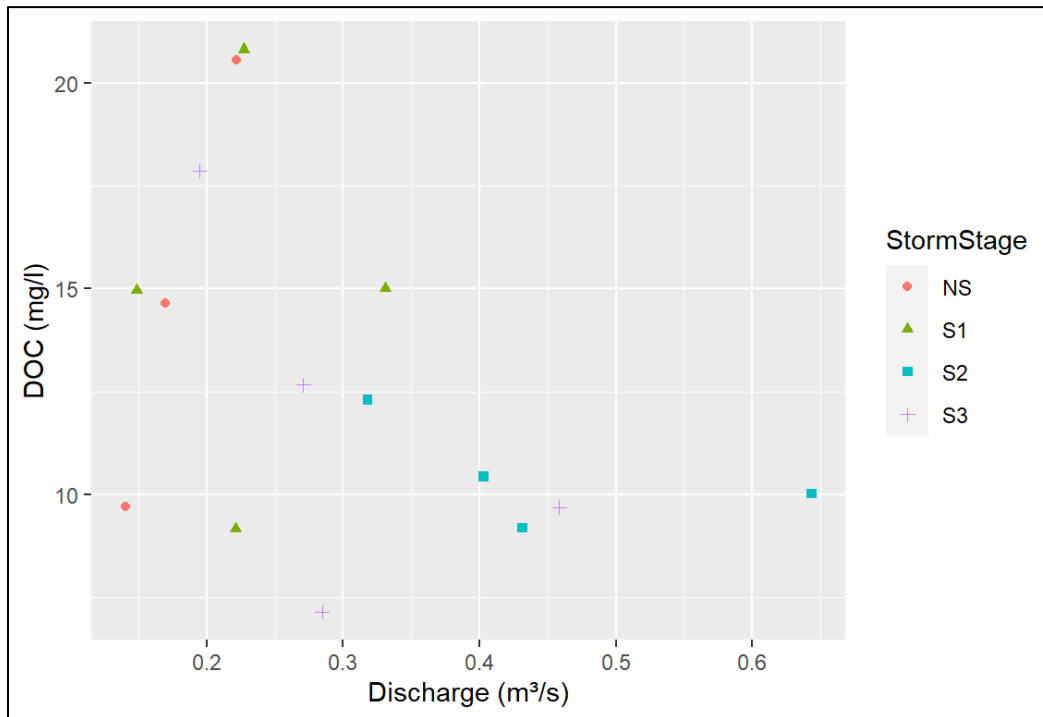
DOC

The mean concentration of DOC was 12.9 mg/l, the σ was 4.26 mg/l, and ranged from 7.1 mg/l to 20.8 mg/l (Table 3). It made up 91% of the mean organic carbon concentrations in the samples taken from Snyder Creek. A Shapiro- Wilks test for normality was run on the DOC concentrations and found that they were not normally distributed. As a result, prior to further statistical analysis the data was logarithmically transformed. It was then reassessed and found to have a normal distribution. DOC was slightly negatively correlated with discharge, but this

correlation was not statistically significant ($r = -0.427$, $p = 0.112$). The data did not reveal a statistically significant difference between storm stages and DOC concentration ($F_{3,11} = 1.087$, $p = 0.395$) (Table 4).

Figure 8

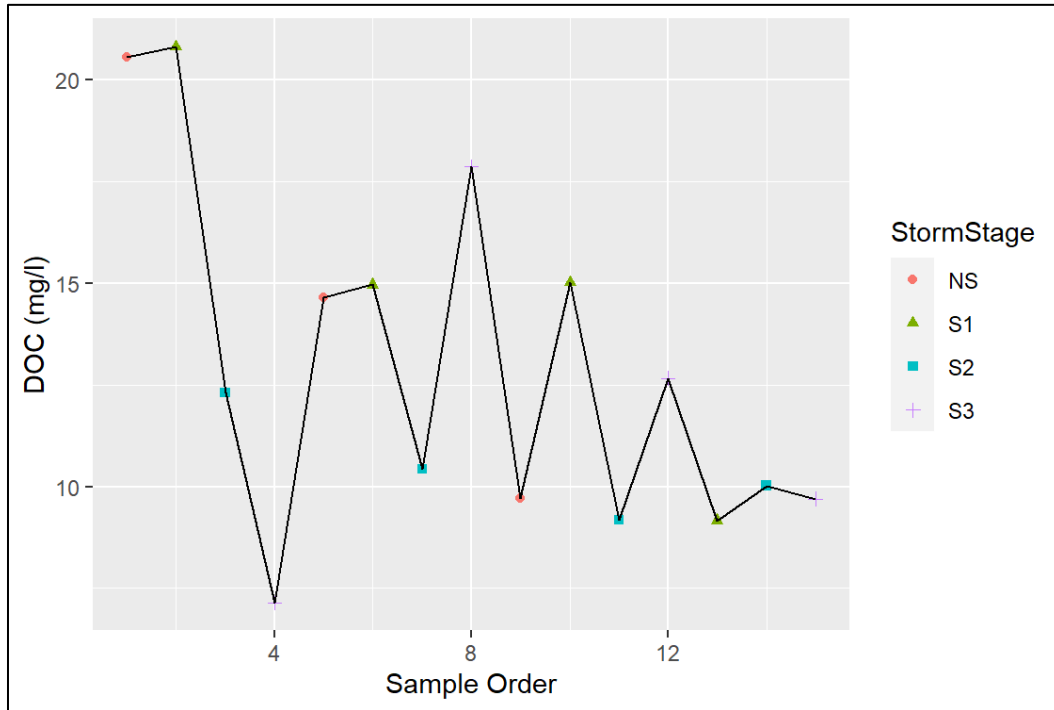
DOC concentrations in Snyder Creek in relation to discharge



The colored symbols represent the stage of the storm that each measurement was taken during.

Figure 9

DOC concentrations in Snyder Creek over the course of the sampling period



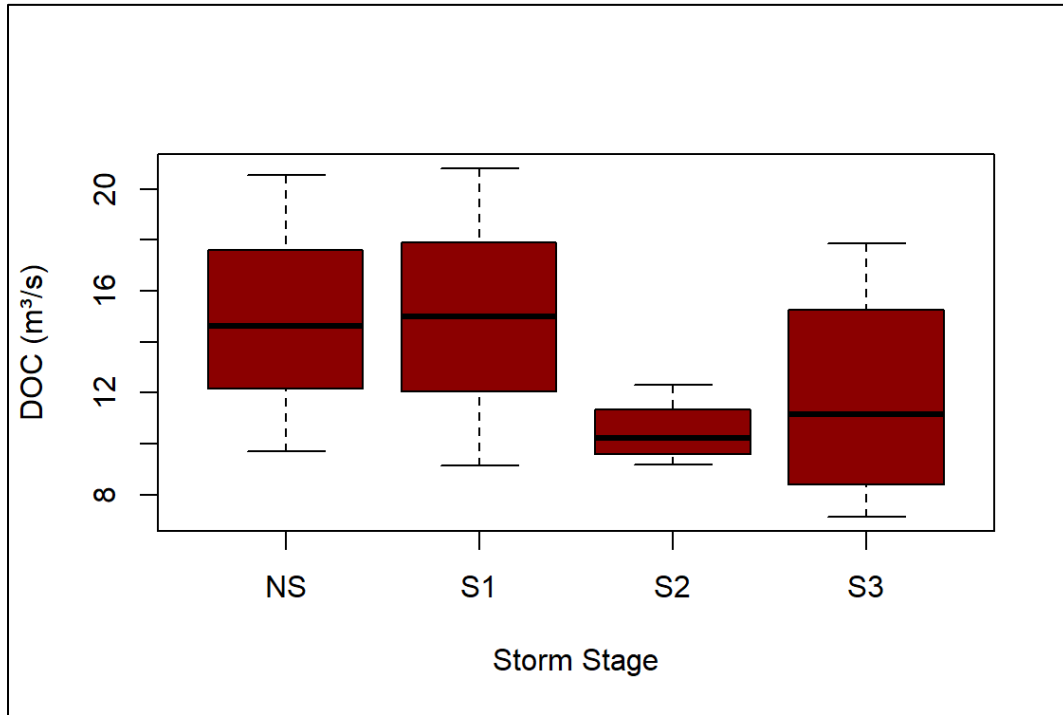
The symbols represent the stage of the storm that each measurement was taken during.

Analysis of the DOC over the sampling window showed a statistically significant moderate negative correlation ($r = -.568$, $p = .027$) between the DOC concentration and the order of the samples taken over the study. This result suggests that as time passes over the course of the spring winter/ sampling window, the DOC concentration decreases (Figure 9).

Another observable pattern in the DOC concentrations was the average standard deviations (σ) between the storm stages (Figure 10). Variability in DOC concentration appears to be the least in the samples taken at the height of the storm (S2) which includes 4 of the 6 highest discharge samples. The S2 samples had a (σ) of 1.141 whereas the σ of all four combined is 3.42.

Figure 10

Box plot of DOC measurements by storm stage



The midpoint represents the median value, the outer edges of the boxes represent the 1st and 3rd quartiles of the data, and the whiskers show the minimum and maximum values.

FPOC

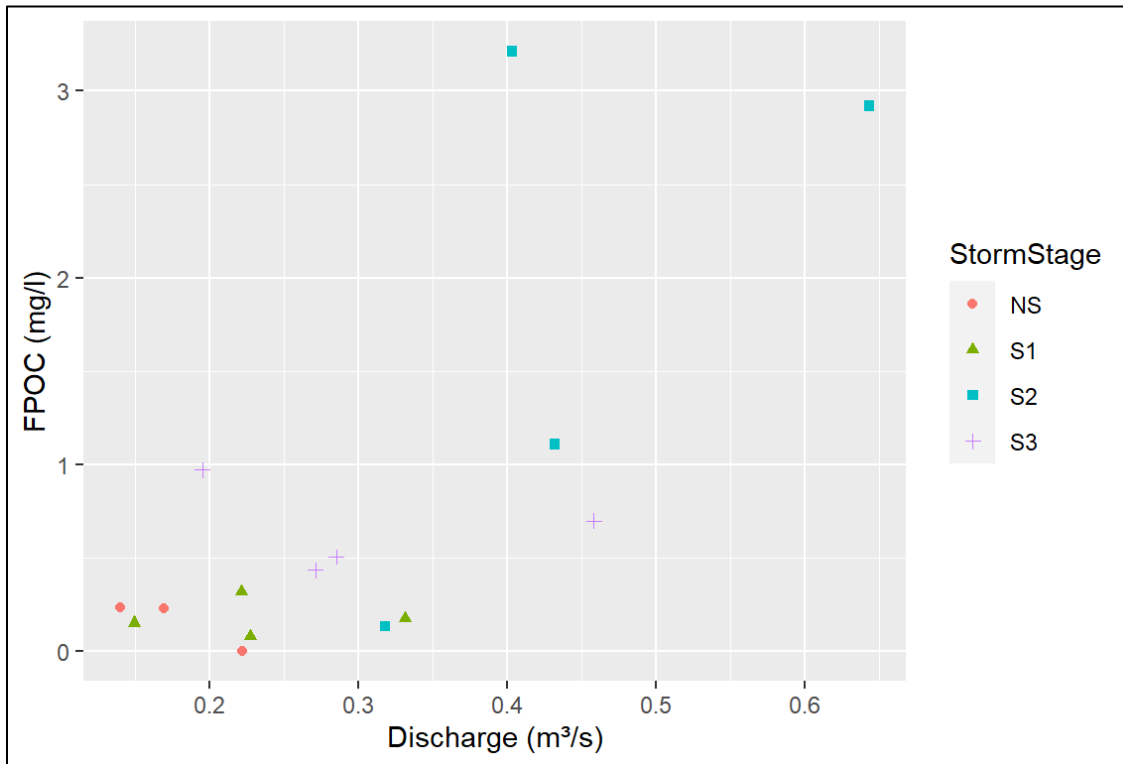
The mean concentration of fine suspended sediment (FSS) samples was 9.86 mg/l, the median was 4.22 mg/l, the σ was 12.96 mg/l, and measurements ranged from 1.85 mg/l to 47.34 mg/l (Table 4). The FSS had a strong positive statistically significant correlation with discharge ($r= 0.625$, $p=0.013$).

The mean concentration of FPOC samples was 0.75 mg/l, the median was 0.32 mg/l, the σ was 0.99 mg/l, and ranged from 0 mg/l to 3.21 mg/l (Table 4). It made up 5% of the mean organic carbon concentrations in the samples taken from Snyder Creek. A Shapiro- Wilks test was run on the FPOC concentration data set and found that it was not normally distributed. A

logarithmic transformation did not result in a normal distribution. As a result, a Spearman’s rank correlation analysis was used instead of a Pearson’s correlation. FPOC had a moderately positive correlation with discharge, this positive correlation was driven by concentrations at the height of the storms (S2) ($r=0.50$, $p= 0.058$) (Figure 11). However, the p-value was greater than 0.05 and cannot be considered statistically significant. Analysis of the FPOC over the sampling window did not show a statistically significant correlation ($r= -0.36$, $p=0.19$) between the FPOC concentration and the order of the samples taken over the study (Figure 12).

Figure 11

FPOC concentrations in Snyder Creek in relation to discharge



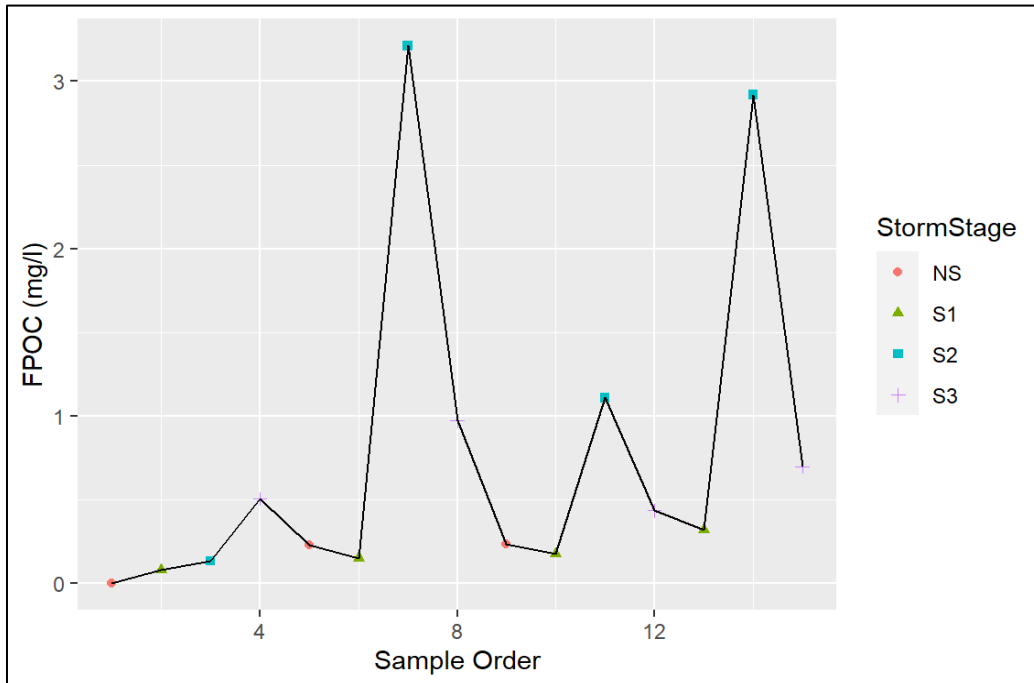
The colored symbols represent the stage of the storm that each measurement was taken during.

A non-parametric Kruskal-Wallis indicated there was no statistically significant difference between storm periods and FPOC concentration ($p=0.067$). However, an observable

pattern in the FPOC concentrations was that the average standard deviations (σ) of FPOC concentrations for NS, S1, and S3 were all under 0.25 mg/l, but the σ of S2 was 1.47 (Figure 12). Additionally, the mean of S2 concentrations was 1.84 mg/l compared to the other storm stages which were all below 0.66 mg/l (Figure 12).

Figure 12

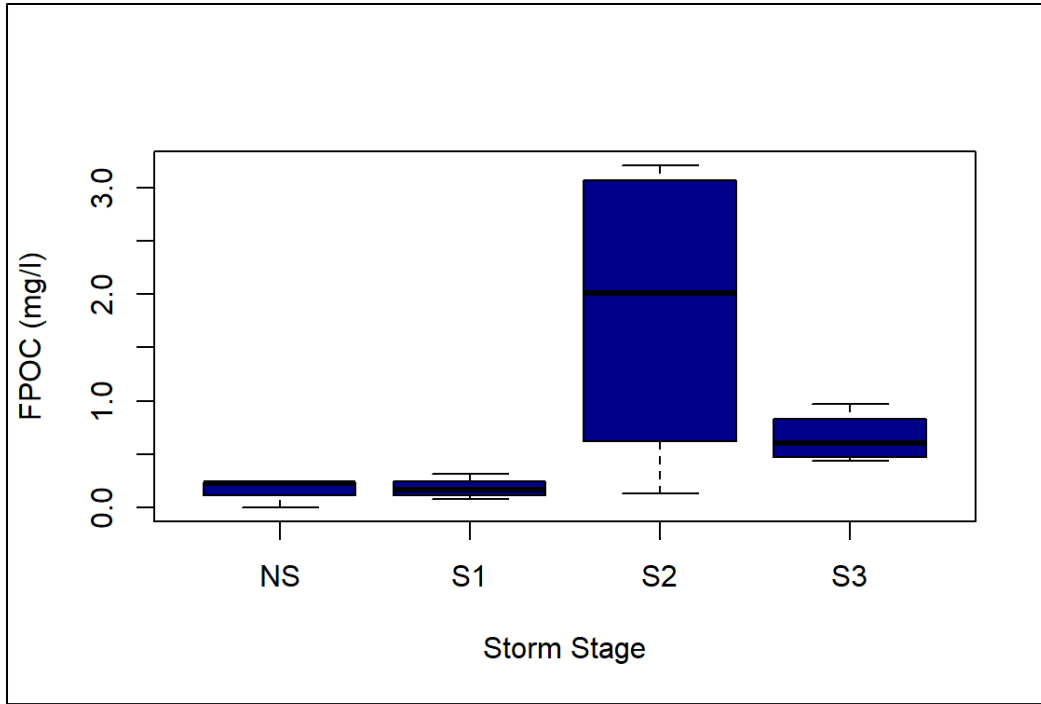
FPOC concentrations in Snyder Creek over the course of the sampling period



The symbols represent the stage of the storm that each measurement was taken during.

Figure 13

Box plot of FPOC measurements by storm stage



The midpoint represents the median value, the outer edges of the boxes represent the 1st and 3rd quartiles of the data, and the whiskers show the minimum and maximum values.

CPOC

Coarse suspended sediment (CSS) samples had a mean concentration of 3.35 mg/l, with a σ of 2.93 mg/l, and a range of 0.32 mg/l to 8.86 mg/l (Table 3). There was not a statistically significant correlation between the coarse suspended sediment (CSS) concentrations and discharge ($r= 0.035$, $p=.899$).

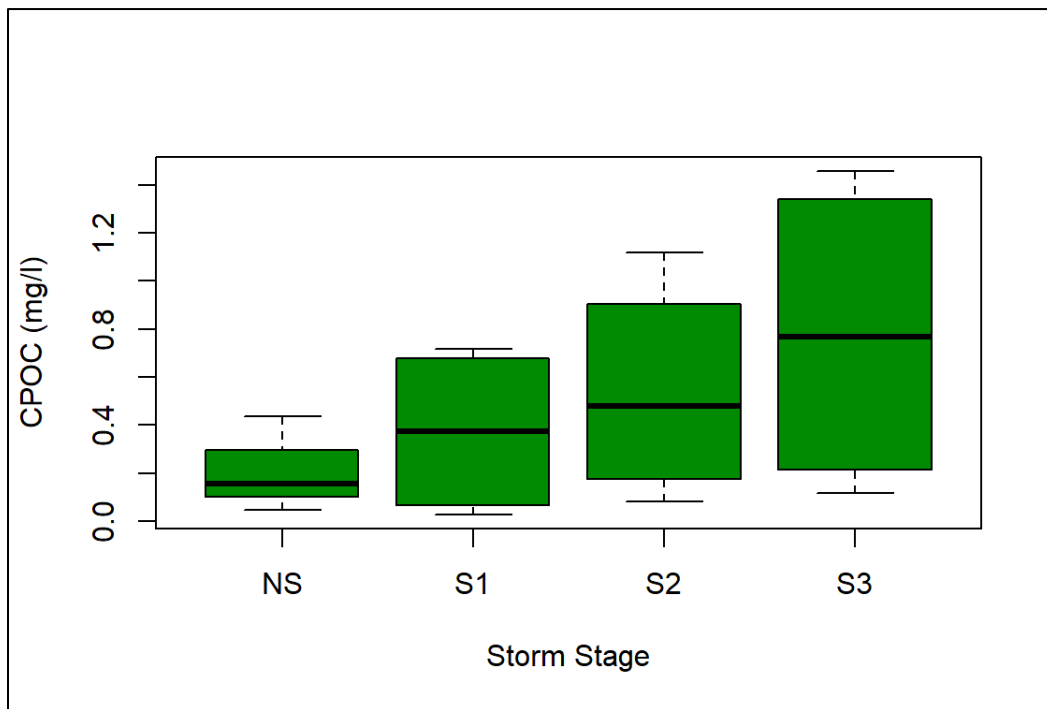
The coarse particulate organic carbon (CPOC) samples had a mean concentration of 0.49 mg/l, with a σ of 0.47 mg/l, and a range of 0.03 mg/l to 1.46 mg/l and (Table 3). There was not a statistically significant difference between the CPOC concentration by storm stage ($F_{3,11}=0.954$, $p=0.448$). However, the mean increased from non- storm stages (NS) to the rising storm stages (S1), to the height of the storms (S2), to the receding storm stages (S3) (Figure 14). The standard

deviations (σ) of the storm stages followed the same pattern (NS=0.20, S1=0.36, S2=0.46, S3=0.66).

CPOC concentrations did not show any correlation between CPOC concentrations and discharge ($r = 0.026, p = 0.448$). There was also not a statistically significant correlation between sample order (time) ($r = 0.129, p = 0.646$).

Figure 14

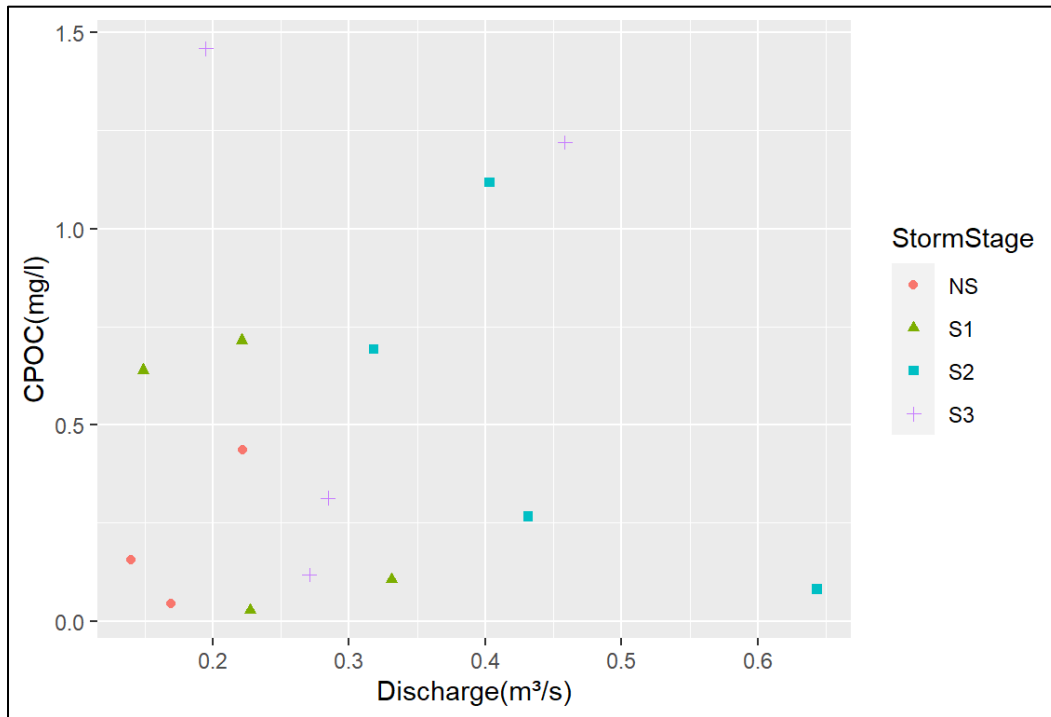
Box plot of CPOC measurements by storm stage



The midpoint represents the median value, the outer edges of the boxes represent the 1st and 3rd quartiles of the data, and the whiskers show the minimum and maximum values.

Figure 15

Graph of the relationship between CPOC concentrations in Snyder Creek and discharge



The graph shows the relationship between CPOC concentrations in Snyder Creek and discharge. The colored symbols represent the stage of the storm that each measurement was taken during.

DIC

Table 5

Snyder Creek stream chemistry and DIC concentrations

Date	Storm Period	pH	Temp (C)	Q (m ³ /s)	Alkalinity (μeq/kg)	DIC (μmol/kg)	
28-Feb	NS	7.44	8.4	0.222	1322.93	1460.88	
12-Mar	S1	7.41	8.4	0.227	1108.17	1232.87	
22-Mar	NS	7.35	9.9	0.169	1339.09	1483.52	
31-Mar	S2	7.17	9.3	0.403	610.94	746.98	
5-Apr	NS	7.44	8.9	0.14	1332.49	1487.35	
7-Apr	S3	7.34	10	0.271	888.21	1071.75	
9-Apr	S2	NA	11.1	0.643	541.02	666.82	
Date	Storm Period	F (μmol CO ₂ /m ² /s)	H ₂ CO ₃	HCO ₃	CO ₃	pCO _{2wa}	pCO _{2atm}
28-Feb	NS	17.768	138.82	1320.584	1.173	2448.194	427.3
12-Mar	S1	18.623	125.63	1106.351	0.911	2215.585	442.18
22-Mar	NS	18.884	145.759	1336.774	1.160	2707.473	445.31
31-Mar	S2	25.583	136.13	610.425	0.258	2477.023	428.08
5-Apr	NS	19.015	155.604	1330.357	1.066	2792.435	431.79
7-Apr	S3	15.648	91.731	886.590	0.811	1709.434	425.93
9-Apr	S2	30.816	125.881	540.578	0.221	2435.268	426.64

Snyder Creek temperatures, pH, discharge, inorganic C species concentrations, and outgassing (F) rates over the course of the study stage.

The mean DIC (TCO₂) value was 1164.31 μmol/kg, with a σ of 348.6 μmol/kg, and a range of 666.8 μmol/kg to 1487.3 μmol/kg (Table 5). DIC concentration in Snyder has a statistically significant strong negative correlation with discharge, ($r = -0.91$, $p = 0.004$). The DIC concentration did not have a significant relationship with sampling order/ time, ($r = -.598$, $p = 0.156$) (Table 6).

Table 6

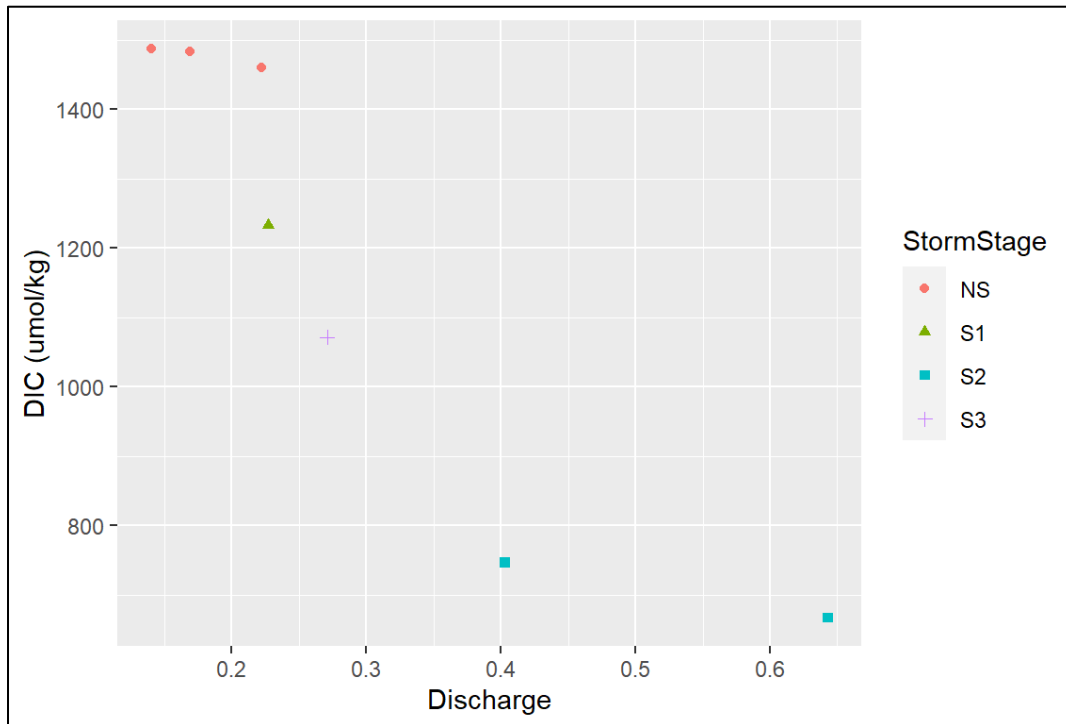
Pearsons R results for multiple variables' relationship to DIC.

Test	Discharge	Sample Order	pH	DOC	FPOC	CPOC
Pearsons R	-0.91	-0.598	0.872	0.480		-0.392

Orange highlights signify statistically significant p-values with moderate to strong correlation coefficients.

Figure 16

Relationship between DIC concentrations in Snyder Creek and stream discharge



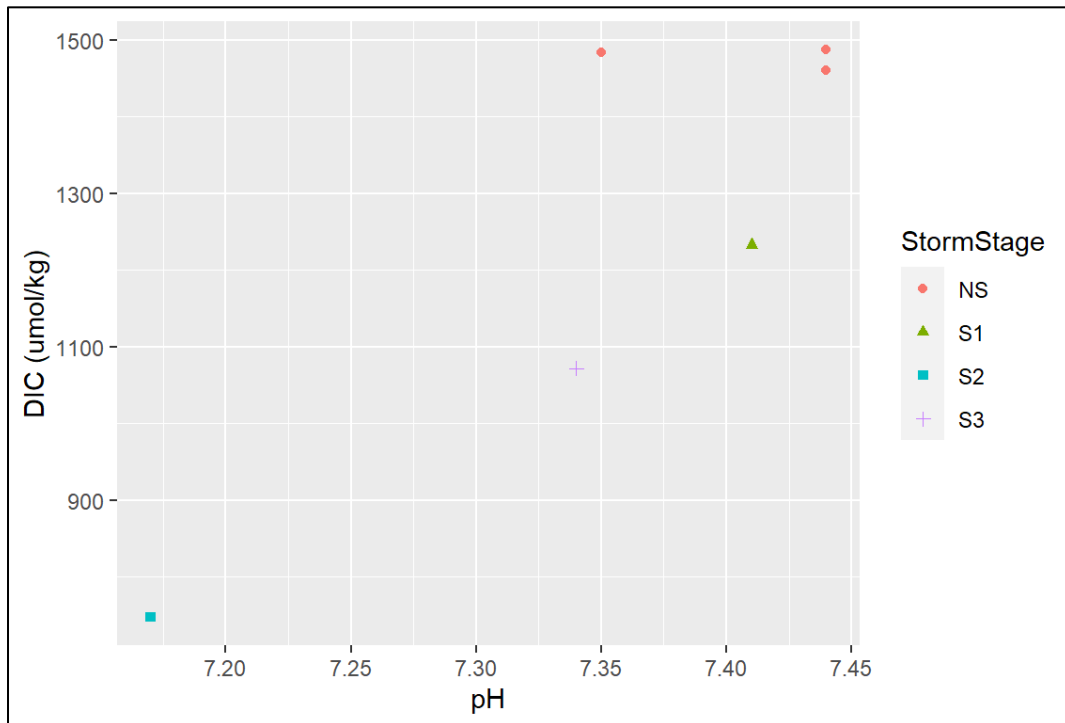
The colored symbols represent the stage of the storm that each measurement was taken during.

There was not a statistically significant relationship between DIC and any of the organic carbon concentrations. There was a moderate correlation between DIC and DOC; however, it was not statistically significant ($r=0.479$, $p=0.276$).

DIC had a strong statistically significant positive correlation with pH ($r= 0.872$, $p=.024$) (Figure 17). pH also has a positive correlation with the percentage of DIC made up of HCO_3^- ($r=0.817$, $p=0.047$), conversely it has a strong negative correlation with the percentage of DIC made up of H_2CO_3 ($r=-0.874$, $p=0.023$). Both relationships can be attributed to the controls of pH on carbonate speciation. This means that as discharge increases, DIC decreases, and the proportion of H_2CO_3 decreases relative to the other carbonate species.

Figure 17

Relationship between DIC concentrations in Snyder Creek and pH



The colored symbols represent the stage of the storm that each measurement was taken during.

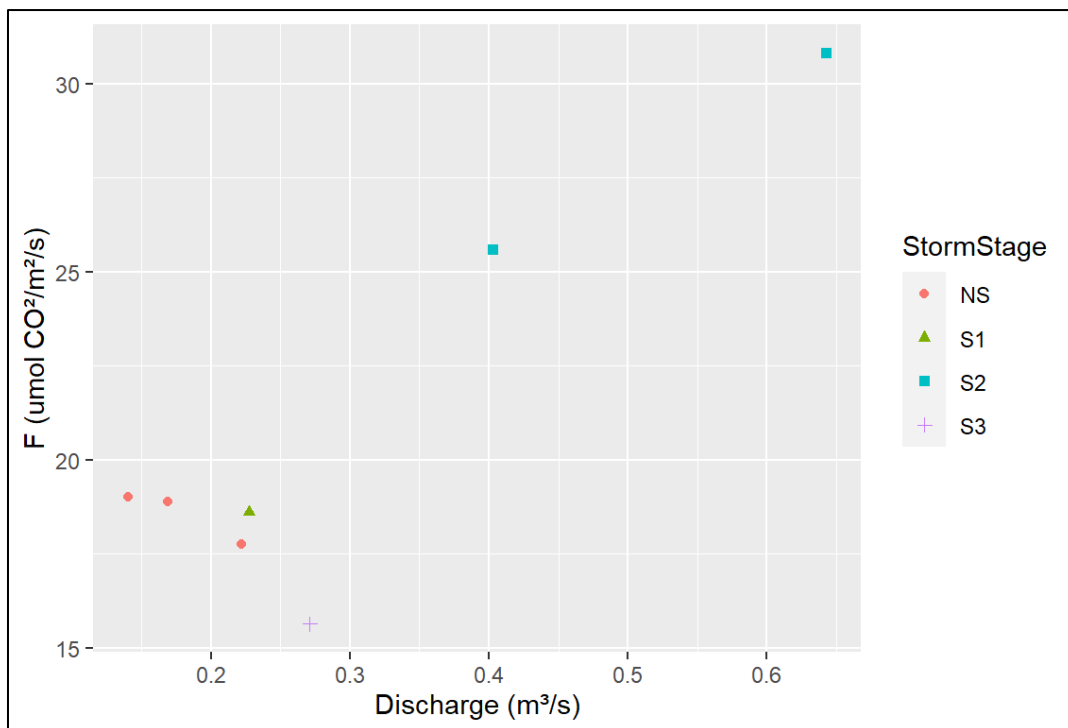
CO₂ Evasion Rates

The mean in-stream CO₂ evasion rate was 20.91 $\mu\text{mol CO}_2 \text{ m}^{-2} \text{ s}^{-1}$, the σ was 5.33, with a range 15.65 $\text{m}^{-2} \text{ s}^{-1}$ to 30.62 $\text{m}^{-2} \text{ s}^{-1}$. Stream Discharge had a strong statistically significant positive correlation with the CO₂ evasion rates ($r= 0.897$, $p= 0.0062$) (Figure 18). This suggests that as discharge increases, outgassing (F) increases. This is the opposite of the correlation between discharge and DIC. An analysis on the relationship between DIC and F shows a strong negative correlation between DIC and outgassing ($r=-.784$, $p= .037$).

The mean partial pressure of aqueous CO₂ in Snyder Creek was 2,3998 (μatm) and the mean partial pressure of atmospheric CO₂ was 432.5 (μatm) (Table 5). This means that Snyder Creek is supersaturated with CO₂ and has approximately five and a half times that of the surrounding atmosphere.

Figure 18

CO₂ outgassing rate in Snyder Creek in relation to stream discharge



The symbols represent the stage of the storm that each measurement was taken during.

Discussion

Discharge

The goal of this study was to see how carbon concentrations changed during storm events and in relation to discharge fluctuations. Four storm events were captured in which discharge (Q) measurements were collected at distinct stages of the hydrograph. During these storm events, the mean discharge of the measurements taken at the height of the storm were the greatest, the non-storm measurements were the lowest, and the rising and falling periods fell between the two. Measurements taken at the peak of the storm (S2) were significantly different from those taken at non-storm stages (NS), and rising storm stages (S1) (Table 1, Figure 6). There were not statistically significant differences in Q between the other storm stages. A possible explanation is that measurements taken for each storm stage did not occur at the same point within each stage (further explanation can be found in the methods section). Another explanation for these results is that the storms varied greatly in the amount of precipitation that fell, which explains the variance in Q between the same stage of different storms.

The mean discharge in Snyder Creek measured during the sampling times increased from February 28th to April 10th. This was shown by a statistically significant moderate positive correlation between the order that the samples were taken and discharge (Figure 7). Additionally, the magnitude of the storm events increased with each storm throughout the study period, as did the change in discharge between the low water measurements and the peak measurements (Figure 8). However, the limited sample size in the study only represents a snapshot of discharge between February 28th and April 10th in Snyder Creek. The sampling dates were also not evenly distributed over the course of the study and only included one non-storm measurement between

storms. These results are most useful for analyzing discharge's relation to carbon concentrations in Snyder Creek as opposed to seasonal discharge trends.

Longer term studies on streams in the region with rain dominant hydrology have shown an overall negative trend in discharge over the same time of year (Giesbrecht et al., 2022). A study on eight small low- order streams located at low elevations within the Puget Sound area exhibited decreasing discharge starting in January that reached a minimum in the summer (Giesbrecht et al., 2022). However, the winter and spring seasons had multi-storm periods of increasing discharge within the larger trend of decrease (Giesbrecht et al., 2022; Argerich et al., 2015). It is possible that the positive trend in discharge measured in Snyder Creek is an example of the multi-storm discharge increases seen in other streams within an overall seasonal decline.

DOC

The mean DOC concentration in Snyder Creek was 12.9 mg/l, the lowest concentration recorded was 7.1 mg/l and the highest was 20.8 mg/l (Table 3, Figure 10). These concentrations are higher than DOC concentration found in similar streams (Giesbrecht et al., 2022). A 2022 meta study on DOC concentrations showed that eight low elevation, low order streams in the Puget Sound area had mean monthly DOC concentrations between ~2.5 mg/l and ~5.5 mg/l for February, March, and April (Giesbrecht et al., 2022). The concentrations reported here were higher than most of the streams in Pacific Northwest creeks and rivers included in the 2022 Giesbrecht study as well as streams included in other studies done in the region (Voss et al., 2015; Argerich et al., 2022). The streams included in the Giesbrecht meta study that had a similar range of DOC concentrations to those reported in this study were located further north in southwestern British Columbia. However, they were about 3°C cooler on average than the streams studied here, resulting in less evapotranspiration. The Snyder Creek temperatures,

however, were within the range of the streams located near Puget Sound and were warmer than temperatures found in these northern streams during the winter season.

A possible reason for significantly higher DOC concentrations in Snyder Creek compared to those in similar watersheds is soil characteristics (Nelson et al., 1992; Butman et al., 2019). Watersheds with soil with higher clay content often adsorb more C and hold onto it during storm pulses (Nelson et al., 1992). Watersheds with sandier soil leaches more DOC into the stream because there is less sorption of this organic matter onto sand particles (Nelson et al., 1992; Butman et al., 2019.) In addition to texture, the presence of poorly crystalline iron (FE_{pc}) and aluminum (Al_{pc}) make a major impact on the DOC sorption in soil (Kothwala & Hendershot, 2009). Carbon: nitrogen ratios in soil can also have a large control on DOC fluxes in streams, with higher C:N ratios typically resulting in higher DOC exports (Aitkenhead- Peterson et al., 2005). Using a soil type map provided by USGS, Snyder Creek watershed contains three soil types, one of which is characterized as being anthropogenically influenced and can be very sandy (Figure 5) (Soil Survey Staff, N.D.). This soil type is unique to watersheds in developed areas such as Snyder Creek which could influence the in-stream storm DOC concentrations. It is difficult to know if soil properties are behind the high DOC concentrations without soil analyses, however they are an important control on stream DOC concentrations and could provide an answer (Camino-Serrano et al., 2014; Nelson et al., 1992; Strawn et al., 2021; Kothwala & Hendershot, 2009; Bianchi et al, 2011).

The Snyder Creek watershed encompasses forested and residential land, with the headwaters starting on the Evergreen State College campus (WFC, 2007). In addition to the type of soil found in this watershed, human caused changes may impact DOC concentrations in Snyder Creek in other ways as well. A 2019 study in Delaware found that anthropogenic changes

to an ecosystem increase the aromaticity of DOC, allowing for an increase in variability in DOC concentrations in streams (Parr et al., 2019). The addition of chemicals, particularly nitrogen and sodium, by humans to promote garden and lawn growth within a watershed can result in increased DOC concentrations in streams (Aitkenhead-Peterson et al., 2009; Aitkenhead Peterson et al., 2005). The introduction of wastewater into a stream in urban areas can also cause increased DOC levels (Tank et al., 2018; Aitkenhead Peterson et al., 2005) Further analysis is needed to determine if human caused changes to the watershed resulted in the heightened DOC concentrations in Snyder Creek, however results from studies on the topic suggest this is a realistic possibility (Parr et al., 2019, Tank et al., 2018; Aitkenhead-Peterson et al., 2009; Aitkenhead Peterson et al., 2005).

Other studies that measured stream DOC concentrations in relation to discharge have found that as discharge increases rapidly in late winter to spring, DOC initially increases, but then begins to decline prior to the height of discharge (S2) measurement (Voss et al., 2016; Argerich et al., 2015; Marx et al., 2017). This can be explained by the depletion of built-up organic matter in a watershed, as it is flushed from the watershed by rain (Marx et al., 2017). This pattern is most apparent on a seasonal timeline (three to six months), although this pattern is also observed for individual storms (Voss et al., 2016; Argerich et al., 2015; Demars et al., 2018; Giesbrecht et al., 2022). The correlation between DOC and discharge is found to be positive in most stream watersheds especially in the winter and spring seasons (Voss et al., 2016; Ward et al., 2017; Raymond et al., 2016). This pattern was not observed in Snyder Creek, as there was a weak negative correlation between discharge and DOC concentrations, without statistical significance (Figure. 8). As with all of the results in this study this finding could be attributed to

the relatively small sample size and perhaps not a fine enough resolution of sampling during storm events to capture this pattern.

There were not statistically significant differences in DOC concentrations between stages of the storm hydrograph (S1, S2, and S3). However, there was a notable difference between their standard deviations. Particularly the concentration at the height of the storm (S2) had a standard deviation (σ) of 1.14 mg/l which is far less than the σ of the other stages of the storm hydrograph (NS=4.44 mg/l, S1=4.12 mg/l, S3=3.99 mg/l). As mentioned previously the largest standard deviation of discharge was in the discharge measurements from the height of the storm. An explanation for the small variance in DOC despite the large variance in discharge at the S2 stage is a result of exhausted DOC sources at high peak discharges (Voss et al., 2016; Argerich et al., 2015; Marx et al., 2017). The relatively large variance in the other stages of the hydrograph (S1, S3) may have influenced the lack of a statistically significant difference between DOC concentrations at the height of the storm (S2) and the other periods. Although these larger σ may be associated with the study design and the inexact timing of the sampling, the discharge results do not support this. It is possible that the reason for the large variation in standard deviations and lack of statistically significant difference between DOC and storm period is associated with the seasonal changes in concentration.

The one variable tested that showed a significant correlation with DOC concentration was the order/ date of the sample. Statistical tests revealed that as time elapsed over the course of the study the DOC concentrations decreased ($R = -.513$, $R^2 = .206$, $P = .05$). Due to the limited samples and study design which target storms, this result does not represent the trend of total DOC concentrations over the course of study period. However, this trend in DOC over the month of March and early April does align with the results from some studies that measured discharge in

small streams in the Pacific Northwest (Argerich et al., 2016, Giesbrecht et al., 2022). The multi-year study by Argerich et al. in Western Oregon revealed a steady decrease in DOC starting in March and ending in July. The comprehensive study carried out by Giesbrecht et al. in 2022 reported that the mean DOC in the low elevation Puget Sound region steadily decreased each month from November to May. This is a result of the depletion of DOC sources and seasonal decrease in discharge (Giesbrecht et al., 2022). Other headwater streams in the Pacific Northwest that are more influenced by snowmelt and glacial run off show peaks in DOC later in the spring right before discharge peaks in the early summer (Voss et al., 2015, Voss et al., 2022, Giesbrechet et al., 2022).

FPOC

The mean concentration of FPOC was 0.75 mg/l and made up 5% of the mean organic carbon concentrations in the samples taken from Snyder Creek, 1% more than CPOC. The greater FPOC concentrations are likely due to the large influxes during the storms (Figure 11). This pattern is common for FPOC concentrations which are typically low during base flow but see major increases during storm pulses (Marx et al., 2017). FPOC is more mobile than CPOC due to its size allowing for this fraction of carbon to be mobilized by less discharge (Marx et al., 2017; Argerich et al., 2016). The proportions of organic carbon were similar to other low order streams in the Pacific Northwest; however, areas with larger storm events and snow melt will sometimes see higher mean CPOC concentrations (Argerich et al., 2016). In Snyder Creek, concentrations spiked during all four storms and were highest during the peak storm stage for the latter three storms. The peak storm stages (S2) of the storms which were three times greater than the concentrations found during the other storm stages (Figure 11, Figure 12). The three greatest concentrations occurred during peak stages even though the second highest discharge recorded

occurred during a falling storm stage (Figure 11). This result points to the mobility of FPOC and the flushing effect of peak discharge (Marx et al., 2017; Tank et al., 2018). Despite this, there was not a statistically significant difference between storm stages ($p=0.07$). This result was likely influenced by the first storm which had lower FPOC concentrations than the other storms and concentrations peaked at the falling storm stage (S3), as compared to the other stages measured here. The first storm also had the smallest increase in discharge.

The mobilization of the FPOC concentrations only at the peak stages of the storms likely influenced its correlation with discharge which was moderate and not statistically significant ($r=0.504$, $p=0.058$). Other than samples collected during the highest discharges, the concentrations were similarly low among all samples. It appears that significant increases in FPOC concentrations did not occur until discharge surpassed a discharge of roughly $0.4 \text{ m}^3/\text{s}$ (Figure 11). However, additional sampling would be needed to determine if this observation is statistically significant.

FPOC concentrations did not have a correlation with sampling order ($r=-0.36$, $p=0.19$). Although discharge at the peak storm stage increased with each storm, FPOC did not follow the same trend. The highest spike in FPOC occurred during the second storm (3.2 mg/l), the third storm saw three times less FPOC (1.18 mg/l) and then climbed back to (2.92 mg/l) at the peak of the fourth storm. The reason for this dip in FPOC was likely caused by the exhaustion of FPOC sources by the second storm (Marx et al., 2017).

CPOC

The CPOC concentrations for Snyder creek had a mean of 0.49 mg/l C with a standard deviation of 0.466 mg/l , that ranged from 0.027 mg/l to 1.459 mg/l over the course of the fifteen

sampling dates (Table 3). The mean CPOC concentration accounts for 4% of the total OC concentrations. This percentage is on par with the annual CPOC concentrations for similarly characterized streams but is low for this time of year when concentrations are at or near their peak (Marx et al., 2017, Argerich et al., 2016). Possible explanations for the lower CPOC concentration include watershed/ creek slope, discharge, and lack of petrogenic sources (Tank et al., 2018, Marx et al., 2017). The moderate slope of the watershed and creek bed as well as moderate discharge pulses recorded at Snyder Creek could explain the lack of correlation between POC and discharge (Marx et al., 2017). These characteristics are the predominant forces that control erosion and consequently biogenic POC influxes (Tank et al., 2018, Marx et al., 2017).

Coarse particulate OC is typically less dynamic in all river systems than smaller fractions of C but is most mobile during high discharge events (Tank et al., 2018). During rapid large increases in discharge, CPOC export often occurs at a greater rate than smaller C fractions (Tank et al., 2018, Marx et al., 2017). This pattern, however, was not present in the CPOC concentrations in Snyder Creek (Figure 12, Figure 13). There was not a statistically significant relation with discharge ($P=.448$, $\text{adj } R^2=-0.076$, $R= 0.026$) or with sample order ($P=0.646$, $\text{adj } R^2=-0.059$, $R=0.129$) meaning that mean discharge did not change over the course of the study. The mean and max CPOC concentrations of each storm stage did increase over the course of the hydrograph however there was not a statistically significant difference between the stages of the storm hydrograph (Figure 11). This indicates that CPOC concentrations were being mobilized with increased discharge, but larger storms may be necessary to see statistical significance (Tank et al., 2018; Marx et al., 2017). The continued rise in mean CPOC concentrations past the peak

storm stage (S2) and into the falling stage of the storm (S3) may suggest that CPOC was mobilized or flushed at a slower rate than discharge fluctuated.

DIC

DIC concentrations in Snyder Creek had a strong inverse relationship with discharge ($R=-0.91$, adj. $R^2=0.828$, $P=0.004$). This is consistent with most streams of similar sizes, locations, and elevations but not all (Demars et al., 2019; Argerich et al., 2016; Wallin et al., 2016). The relationship found in Snyder Creek is likely due to the dilution of DIC sources (e.g. DIC in soil and instream respiration) with increasing precipitation and short residence time due to higher discharges (Argerich et al., 2016). CO_2 outgassing had an inverse relationship with DIC concentration (expanded upon below), a trend that was observed in similar watersheds. The data also showed that although the DIC concentrations taken during storms decreased (discharge increased) over the course of the study, the non-storm (NS) DIC concentrations stayed constant. This suggests that the sources of DIC were not depleted by storm pulses and concentrations were able to reaccumulate after being flushed by rapid increases in discharge.

The lowest DIC concentration in Snyder Creek was $666.8 \mu\text{mol/kg}$ taken during the peak stage of the storm and the highest was $1487.35 \mu\text{mol/kg}$ taken during a non-storm period, which is a 123% increase. This range in concentrations over the course of a storm is similar in magnitude to other small streams with rain driven hydrology during this time of year (Demars et al., 2019, Argerich et al., 2016). However due to the longer timeline of most stream C studies in which measurements were only taken once a week to once a month, there were only a couple of studies available that measured DIC concentrations at a similar frequency to this study (Demars et al., 2019; Argerich et al., 2016).

The composition of DIC species in Snyder Creek was made up of a mean of 88% HCO_3^- , 12% H_2CO_3 and <.001% of CO_3^{2-} . The species had relatively consistent values throughout the study period with a standard deviation for H_2CO_3 of $\pm 4\%$. The fluctuations that did occur were strongly correlated with pH. As pH increased, DIC concentrations increased ($R = 0.872$, $R^2 = 0.7$, $P = .024$) as did the proportion of DIC made up of HCO_3^- , and the proportion of H_2CO_3 decreased ($R = -0.874$, $R^2 = 0.704$, $P = 0.023$). This correlation pattern reflects the controls that pH has on carbonate system speciation particularly in small low order streams (Wallin et al., 2010). The proportion of HCO_3^- to H_2CO_3 is also consistent with small headwater streams that have relatively high pH levels (>7) (Marx et al., 2017). The low carbonate concentrations suggest that Snyder Creek DIC is mostly sourced from biotic respiration and some carbonate dissolution, with little silicate dissolution (Marx et al., 2017; Wallin et al., 2010).

CO₂ Outgassing

In stream CO_2 partial pressure ($\text{pCO}_{2\text{wa}}$) calculations were an average of 4.5 times the $\text{pCO}_{2\text{atm}}$ measured at the Nannoos Orca buoy by NOAA's Pacific Marine Environmental Laboratory (Table 6). It is important to note that the buoy is located ~40 miles from the sampling site, and therefore the $\text{pCO}_{2\text{atm}}$ levels are not exact and are only used as an approximation. This level of excess CO_2 partial pressure of CO_2 falls within the range of saturation in small low order streams in the Pacific Northwest (Argerich et al., 2016; Ward et al., 2017; Demars, 2017). The rate of CO_2 outgassing (F) in Snyder Creek had a strong positive correlation with discharge ($R = .897$, $P = .0062$) (Figure 18). This result is in line with the majority of studies on stream CO_2 outgassing rates, which also tend to be positively correlated with discharge (Demars et al., 2019, Raymond et al., 2016). Consequently, there was a strong negative correlation between the outgassing rate and the DIC concentration in Snyder Creek ($P = 0.037$, $\text{adj. } R^2 = 0.54$, $R = -0.784$).

This shows that as discharge increases, and DIC decreases, CO₂ outgassing increases. Previous studies on small streams show comparable results (Demars et al., 2019; Raymond et al., 2016). Although seasonal DIC concentrations increase in the winter and spring season, source limitations can result in decreasing concentrations during rapid storm fluxes (Demars, 2019).

In most stream studies, increased discharge during storm events resulted in decreased DIC concentrations and pH; however, pCO_{2wa} concentrations rose resulting in increased outgassing (F) (Demars, 2017; Almeida et al., 2017). Despite decreased DIC and pH and increased F, PCO_{2wa} did not increase in this study during storm events. In Snyder Creek there was a low proportion H₂CO₃ in DIC even at high discharge, when it increased. It is likely that the model used is the reason why F increased with discharge, because the model calculates the gas transfer coefficient as a function of velocity (Alin et al., 2012). More specifically, the gas transfer coefficient is positively correlated with water velocity, which likely led to the increased outgassing rates at high discharges. To obtain precise pCO_{2wa} and F figures in Snyder Creek, infield measurements would need to be made for better estimates of the gas transfer coefficient.

In addition to DIC outgassing, stream respiration of DOC can make a major impact on CO₂ outgassing (Demars et al. 2019). There was not an observable or statistically significant relationship between DOC and outgassing. One sign of substantial DOC respiration is that peak outgassing is reached after peak discharge during the falling storm stage (Demars et al., 2019). The data does not show that this is occurring in Snyder, but the small amount of outgassing data could be obscuring this.

Conclusion

There were three main findings in this study that either raised questions about the future of C cycling in Snyder Creek and/or differed from other low order streams in the Pacific Northwest. Firstly, despite a lack of statistical significance, the high FPOC concentrations at the peak stage of the storms highlight the impact that increased storm precipitation has on FPOC in Snyder Creek. However, a lower FPOC concentration at the peak of the third storm compared to the second and fourth peaks suggests an exhaustion of the most mobile stocks of this fraction of C. This raises the question; will more precipitation result in significantly more FPOC transported to the stream or will limited FPOC stocks limit stream concentrations? Secondly, mean DOC concentrations in Snyder Creek taken during the study were significantly greater than similarly characterized streams in the region (Giesbrecht et al., 2022). A possible explanation for these results is soil properties and anthropogenic development within the watershed, which would require future soil sampling and analysis to confirm along with DOC analysis. These findings could help to better understand the anthropogenic impacts on carbon cycling within a watershed. Finally, DIC concentration and speciation as well as outgassing were strongly correlated with discharge over the course of the storm hydrograph. These findings, which are in line with the findings in most low order streams, suggest increases in lateral exports and outgassing if storm frequency and intensity increases.

This study revealed initial insight into patterns of carbon concentration fluctuations in Snyder Creek during late winter/ early spring storm pulses that suggest the potential for increased exports in the face of heightened storm discharge. However, it is important that further in-depth research is conducted to determine if the carbon cycling dynamics change during storm pulses that exceed the discharge observed in this study.

References

- Aitkenhead-Peterson, J. A., Alexander, J. E., & Clair, T. A. (2005). Dissolved organic carbon and dissolved organic nitrogen export from forested watersheds in Nova Scotia: Identifying controlling factors. *Global Biogeochemical Cycles*, *19*(4).
<https://doi.org/10.1029/2004GB002438>
- Aitkenhead-Peterson, J. A., Steele, M. K., Nahar, N., & Santhy, K. (2009). Dissolved organic carbon and nitrogen in urban and rural watersheds of south-central Texas: Land use and land management influences. *Biogeochemistry*, *96*(1), 119–129.
<https://doi.org/10.1007/s10533-009-9348-2>
- Argerich, A., Haggerty, R., Johnson, S. L., Wondzell, S. M., Dosch, N., Corson-Rikert, H., Ashkenas, L. R., Pennington, R., & Thomas, C. K. (2016). Comprehensive multiyear carbon budget of a temperate headwater stream. *Journal of Geophysical Research: Biogeosciences*, *121*(5), 1306–1315. <https://doi.org/10.1002/2015JG003050>
- Aufdenkampe, A. K., Mayorga, E., Raymond, P. A., Melack, J. M., Doney, S. C., Alin, S. R., Aalto, R. E., & Yoo, K. (2011). Riverine coupling of biogeochemical cycles between land, oceans, and atmosphere. *Frontiers in Ecology and the Environment*, *9*(1), 53–60.
<https://doi.org/10.1890/100014>
- Bianchi, T. S. (2011). The role of terrestrially derived organic carbon in the coastal ocean: A changing paradigm and the priming effect. *Proceedings of the National Academy of Sciences*, *108*(49), 19473–19481. <https://doi.org/10.1073/pnas.1017982108>
- Blair, N. E., E. L. Leithold, H. Brackley, N. Trustrum, M. Page, and L. Childress. 2010. Terrestrial sources and export of particulate organic carbon in the Waipaoa sedimentary

system: Problems, progress and processes. *Mar. Geol.* 270: 108–118.

doi:10.1016/j.margeo.2009.10.016

Blair, N. E., & Aller, R. C. (2012). The Fate of Terrestrial Organic Carbon in the Marine Environment. *Annual Review of Marine Science*, 4(1), 401–423.

<https://doi.org/10.1146/annurev-marine-120709-142717>

Butman, D. E., Wilson, H. F., Barnes, R. T., Xenopoulos, M. A., & Raymond, P. A. (2015). Increased mobilization of aged carbon to rivers by human disturbance. *Nature Geoscience*, 8(2), Article 2.

<https://doi.org/10.1038/ngeo2322>

Buffam, I., Galloway, J. N., Blum, L. K., & McGlathery, K. J. (2001). A stormflow/baseflow comparison of dissolved organic matter concentrations and bioavailability in an Appalachian stream. *Biogeochemistry*, 53(3), 269–306.

<https://doi.org/10.1023/A:1010643432253>

Burdige, D. J. (2005). Burial of terrestrial organic matter in marine sediments: A re-assessment.

Global Biogeochemical Cycles, 19(4). <https://doi.org/10.1029/2004GB002368>

Camino-Serrano, M., Gielen, B., Luyssaert, S., Ciais, P., Vicca, S., Guenet, B., Vos, B. D., Cools, N., Ahrens, B., Altaf Arain, M., Borcken, W., Clarke, N., Clarkson, B., Cummins, T., Don, A., Pannatier, E. G., Laudon, H., Moore, T., Nieminen, T. M., ... Janssens, I. (2014). Linking variability in soil solution dissolved organic carbon to climate, soil type, and vegetation type. *Global Biogeochemical Cycles*, 28(5), 497–509.

<https://doi.org/10.1002/2013GB004726>

Christensen, J. H., Hewitson, B., Busuioc, A., Chen, A., Gao, X., Held, I., Jones, R., Kolli, R. K., Kwon, W.-T., Mearns, L., Menéndez, C. G., Räisänen, J., Rinke, A., Sarr, A., Whetton,

- P., Arritt, R., Benestad, R., Beniston, M., Bromwich, D., ... Giorgi, F. (2017). *Regional Climate Projections*. 94.
- Cole, J. J., & Prairie, Y. T. (2014). Dissolved CO₂ in Freshwater Systems☆. In *Reference Module in Earth Systems and Environmental Sciences*. Elsevier.
<https://doi.org/10.1016/B978-0-12-409548-9.09399-4>
- Cole, J. J., Prairie, Y. T., Caraco, N. F., McDowell, W. H., Tranvik, L. J., Striegl, R. G., Duarte, C. M., Kortelainen, P., Downing, J. A., Middelburg, J. J., & Melack, J. (2007). Plumbing the Global Carbon Cycle: Integrating Inland Waters into the Terrestrial Carbon Budget. *Ecosystems*, 10(1), 172–185. <https://doi.org/10.1007/s10021-006-9013-8>
- Covino, T. P., McGlynn, B. L., & McNamara, R. A. (2010). Tracer Additions for Spiraling Curve Characterization (TASCC): Quantifying stream nutrient uptake kinetics from ambient to saturation. *Limnology and Oceanography: Methods*, 8(9), 484–498.
<https://doi.org/10.4319/lom.2010.8.484>
- Cui, X., Bianchi, T. S., Jaeger, J. M., & Smith, R. W. (2016). Biospheric and petrogenic organic carbon flux along southeast Alaska. *Earth and Planetary Science Letters*, 452, 238–246.
<https://doi.org/10.1016/j.epsl.2016.08.002>
- Davidson EA, Janssens IA (2006) Temperature sensitivity of soil carbon decomposition and feedbacks to climate change. *Nature* 440:165–173.
- Demars, B. O. L. (2019). Hydrological pulses and burning of dissolved organic carbon by stream respiration. *Limnology and Oceanography*, 64(1), 406–421.
<https://doi.org/10.1002/lno.11048>

- Drake, T. W., Raymond, P. A., & Spencer, R. G. M. (2018). Terrestrial carbon inputs to inland waters: A current synthesis of estimates and uncertainty. *Limnology and Oceanography Letters*, 3(3), 132–142. <https://doi.org/10.1002/lol2.10055>
- Eglinton, T. I., Galy, V. V., Hemingway, J. D., Feng, X., Bao, H., Blattmann, T. M., Dickens, A. F., Gies, H., Giosan, L., Haghypour, N., Hou, P., Lupker, M., McIntyre, C. P., Montluçon, D. B., Peucker-Ehrenbrink, B., Ponton, C., Schefuß, E., Schwab, M. S., Voss, B. M., ... Zhao, M. (2021). Climate control on terrestrial biospheric carbon turnover. *Proceedings of the National Academy of Sciences*, 118(8), e2011585118. <https://doi.org/10.1073/pnas.2011585118>
- Fasching, C., Ulseth, A. J., Schelker, J., Steniczka, G., & Battin, T. J. (2016). Hydrology controls dissolved organic matter export and composition in an Alpine stream and its hyporheic zone. *Limnology and Oceanography*, 61(2), 558–571. <https://doi.org/10.1002/lno.10232>
- Fellows, C. S., Valett, M. H., & Dahm, C. N. (2001). Whole-stream metabolism in two montane streams: Contribution of the hyporheic zone. *Limnology and Oceanography*, 46(3), 523–531. <https://doi.org/10.4319/lo.2001.46.3.0523>
- Galy, V., Peucker-Ehrenbrink, B., & Eglinton, T. (2015). Global carbon export from the terrestrial biosphere controlled by erosion. *Nature*, 521(7551), Article 7551. <https://doi.org/10.1038/nature14400>
- Giesbrecht, I. J. W., Tank, S. E., Frazer, G. W., Hood, E., Gonzalez Arriola, S. G., Butman, D. E., D'Amore, D. V., Hutchinson, D., Bidlack, A., & Lertzman, K. P. (2022). Watershed Classification Predicts Streamflow Regime and Organic Carbon Dynamics in the Northeast Pacific Coastal Temperate Rainforest. *Global Biogeochemical Cycles*, 36(2), e2021GB007047. <https://doi.org/10.1029/2021GB007047>

- Guarch-Ribot, A., & Butturini, A. (2016). Hydrological conditions regulate dissolved organic matter quality in an intermittent headwater stream. From drought to storm analysis. *Science of The Total Environment*, *571*, 1358–1369. <https://doi.org/10.1016/j.scitotenv.2016.07.060>
- Hatfield, J. L., & Dold, C. (2019). Water-Use Efficiency: Advances and Challenges in a Changing Climate. *Frontiers in Plant Science*, *10*. <https://www.frontiersin.org/articles/10.3389/fpls.2019.00103>
- Hatten, J. A., Goñi, M. A., & Wheatcroft, R. A. (2012). Chemical characteristics of particulate organic matter from a small, mountainous river system in the Oregon Coast Range, USA. *Biogeochemistry*, *107*(1), 43–66. <https://doi.org/10.1007/s10533-010-9529-z>
- Hauer & Lamberti. (2007). *Methods in Stream Ecology*. Amsterdam: Elsevier. Print.
- Hedges, J. I. (1992). Global biogeochemical cycles: Progress and problems. *Marine Chemistry*, *39*(1), 67–93. [https://doi.org/10.1016/0304-4203\(92\)90096-S](https://doi.org/10.1016/0304-4203(92)90096-S)
- Heffernan, J. B., & Cohen, M. J. (2010). Direct and indirect coupling of primary production and diel nitrate dynamics in a subtropical spring-fed river. *Limnology and Oceanography*, *55*(2), 677–688. <https://doi.org/10.4319/lo.2010.55.2.0677>
- Hilton, R. G., Galy, A., Hovius, N., Kao, S.-J., Horng, M.-J., & Chen, H. (2012). Climatic and geomorphic controls on the erosion of terrestrial biomass from subtropical mountain forest. *Global Biogeochemical Cycles*, *26*(3). <https://doi.org/10.1029/2012GB004314>
- Hinton, M. J., Schiff, S. L., & English, M. C. (1998). Sources and flowpaths of dissolved organic carbon during storms in two forested watersheds of the Precambrian Shield. *Biogeochemistry*, *41*(2), 175–197. <https://doi.org/10.1023/A:1005903428956>

- Hotchkiss, E. R., Hall Jr, R. O., Sponseller, R. A., Butman, D., Klaminder, J., Laudon, H., Rosvall, M., & Karlsson, J. (2015). Sources of and processes controlling CO² emissions change with the size of streams and rivers. *Nature Geoscience*, 8(9), Article 9. <https://doi.org/10.1038/ngeo2507>
- Jex, C. N., Pate, G. H., Blyth, A. J., Spencer, R. G. M., Hernes, P. J., Khan, S. J., & Baker, A. (2014). Lignin biogeochemistry: From modern processes to Quaternary archives. *Quaternary Science Reviews*, 87, 46–59. <https://doi.org/10.1016/j.quascirev.2013.12.028>
- Johnson, M. S., Lehmann, J., Riha, S. J., Krusche, A. V., Richey, J. E., Ometto, J. P. H. B., & Couto, E. G. (2008). CO₂ efflux from Amazonian headwater streams represents a significant fate for deep soil respiration. *Geophysical Research Letters*, 35(17). <https://doi.org/10.1029/2008GL034619>
- Jones, Jeremy B., Fisher, S. G., & Grimm, N. B. (1995). Nitrification in the Hyporheic Zone of a Desert Stream Ecosystem. *Journal of the North American Benthological Society*, 14(2), 249–258. <https://doi.org/10.2307/1467777>
- Kaplan, L. A., & Newbold, J. D. (2000). 10—Surface and Subsurface Dissolved Organic Carbon. In J. B. Jones & P. J. Mulholland (Eds.), *Streams and Ground Waters* (pp. 237–258). Academic Press. <https://doi.org/10.1016/B978-012389845-6/50011-9>
- Klos, P. Z., Link, T. E., & Abatzoglou, J. T. (2014). Extent of the rain-snow transition zone in the western U.S. under historic and projected climate. *Geophysical Research Letters*, 41(13), 4560–4568. <https://doi.org/10.1002/2014GL060500>
- Kothawala, D. N., Moore, T. R., & Hendershot, W. H. (2009). Soil Properties Controlling the Adsorption of Dissolved Organic Carbon to Mineral Soils. *Soil Science Society of America Journal*, 73(6), 1831–1842. <https://doi.org/10.2136/sssaj2008.0254>

- Kunkel, K. E., Karl, T. R., Easterling, D. R., Redmond, K., Young, J., Yin, X., & Hennon, P. (2013). Probable maximum precipitation and climate change. *Geophysical Research Letters*, 40(7), 1402–1408. <https://doi.org/10.1002/grl.50334>
- Le Quéré, C., Moriarty, R., Andrew, R. M., Peters, G. P., Ciais, P., Friedlingstein, P., Jones, S. D., Sitch, S., Tans, P., Arneeth, A., Boden, T. A., Bopp, L., Bozec, Y., Canadell, J. G., Chini, L. P., Chevallier, F., Cosca, C. E., Harris, I., Hoppema, M., ... Zeng, N. (2015). Global carbon budget 2014. *Earth System Science Data*, 7(1), 47–85. <https://doi.org/10.5194/essd-7-47-2015>
- Leithold, E. L., Blair, N. E., & Perkey, D. W. (2006). Geomorphologic controls on the age of particulate organic carbon from small mountainous and upland rivers. *Global Biogeochemical Cycles*, 20(3). <https://doi.org/10.1029/2005GB002677>
- Luce, C., Staab, B., Kramer, M., Wenger, S., Isaak, D., & McConnell, C. (2014). Sensitivity of summer stream temperatures to climate variability in the Pacific Northwest. *Water Resources Research*, 50(4), 3428–3443. <https://doi.org/10.1002/2013WR014329>
- Masiello C, Druffel E (2001) Carbon isotope geochemistry of the Santa Clara River. *Global Biogeochem Cycles* 15: 407–416
- Medeiros, P. M., Seidel, M., Niggemann, J., Spencer, R. G. M., Hernes, P. J., Yager, P. L., Miller, W. L., Dittmar, T., & Hansell, D. A. (2016). A novel molecular approach for tracing terrigenous dissolved organic matter into the deep ocean. *Global Biogeochemical Cycles*, 30(5), 689–699. <https://doi.org/10.1002/2015GB005320>
- Medeiros, P. M., Sikes, E. L., Thomas, B., & Freeman, K. H. (2012a). Flow discharge influences on input and transport of particulate and sedimentary organic carbon along a small

- temperate river. *Geochimica et Cosmochimica Acta*, 77, 317–334.
<https://doi.org/10.1016/j.gca.2011.11.020>
- Mote, P. W., & Salathé, E. P. (2010). Future climate in the Pacific Northwest. *Climatic Change*, 102(1), 29–50. <https://doi.org/10.1007/s10584-010-9848-z>
- Mulholland, P. J., Tank, J. L., Webster, J. R., Bowden, W. B., Dodds, W. K., Gregory, S. V., Grimm, N. B., Hamilton, S. K., Johnson, S. L., Martí, E., McDowell, W. H., Merriam, J. L., Meyer, J. L., Peterson, B. J., Valett, H. M., & Wollheim, W. M. (2002). Can uptake length in streams be determined by nutrient addition experiments? Results from an interbiome comparison study. *Journal of the North American Benthological Society*, 21(4), 544–560. <https://doi.org/10.2307/1468429>
- Nelson, P. N., Baldock, J. A., & Oades, J. M. (1992). Concentration and composition of dissolved organic carbon in streams in relation to catchment soil properties. *Biogeochemistry*, 19(1), 27–50. <https://doi.org/10.1007/BF00000573>
- Neu, V., Ward, N. D., Krusche, A. V., & Neill, C. (2016). Dissolved Organic and Inorganic Carbon Flow Paths in an Amazonian Transitional Forest. *Frontiers in Marine Science*, 3. <https://www.frontiersin.org/articles/10.3389/fmars.2016.00114>
- Poesen, J., Nachtergaele, J., Verstraeten, G., & Valentin, C. (2003). Gully erosion and environmental change: Importance and research needs. *CATENA*, 50(2), 91–133. [https://doi.org/10.1016/S0341-8162\(02\)00143-1](https://doi.org/10.1016/S0341-8162(02)00143-1)
- Porcal, P., Dillon, P. J., & Molot, L. A. (2015). Temperature Dependence of Photodegradation of Dissolved Organic Matter to Dissolved Inorganic Carbon and Particulate Organic Carbon. *PLOS ONE*, 10(6), e0128884. <https://doi.org/10.1371/journal.pone.0128884>

- Powers, P.D. and C.S. Saunders. (1998). Fish Passage Design Flows for Ungaged Catchments in Washington. *Report by WDFW Lands and Restoration Program, Environmental Engineering Division, Olympia, Washington*
- Raymond, P. A., Hartmann, J., Lauerwald, R., Sobek, S., McDonald, C., Hoover, M., Butman, D., Striegl, R., Mayorga, E., Humborg, C., Kortelainen, P., Dürr, H., Meybeck, M., Ciais, P., & Guth, P. (2013). Global carbon dioxide emissions from inland waters. *Nature*, 503(7476), Article 7476. <https://doi.org/10.1038/nature12760>
- Raymond, P. A., Saiers, J. E., & Sobczak, W. V. (2016). Hydrological and biogeochemical controls on watershed dissolved organic matter transport: Pulse-shunt concept. *Ecology*, 97(1), 5–16. <https://doi.org/10.1890/14-1684.1>
- Regnier, P., Friedlingstein, P., Ciais, P., Mackenzie, F. T., Gruber, N., Janssens, I. A., Laruelle, G. G., Lauerwald, R., Luysaert, S., Andersson, A. J., Arndt, S., Arnosti, C., Borges, A. V., Dale, A. W., Gallego-Sala, A., Godd ris, Y., Goossens, N., Hartmann, J., Heinze, C., ... Thullner, M. (2013). Anthropogenic perturbation of the carbon fluxes from land to ocean. *Nature Geoscience*, 6(8), Article 8. <https://doi.org/10.1038/ngeo1830>
- Roberts, B. J., & Mulholland, P. J. (2007). In-stream biotic control on nutrient biogeochemistry in a forested stream, West Fork of Walker Branch. *Journal of Geophysical Research: Biogeosciences*, 112(G4). <https://doi.org/10.1029/2007JG000422>
- Rosenheim, B. E., Roe, K. M., Roberts, B. J., Kolker, A. S., Allison, M. A., & Johannesson, K. H. (2013). River discharge influences on particulate organic carbon age structure in the Mississippi/Atchafalaya River System. *Global Biogeochemical Cycles*, 27(1), 154–166. <https://doi.org/10.1002/gbc.20018>
- W. H. Schlesinger, E. S. Bernhardt (2013) *Biogeochemistry* (Third Edition). Academic Press.

ISBN 9780123858740, <https://doi.org/10.1016/B978-0-12-385874-0.09991-X>.

Schöning I, Totsche KU, Kögel-Knabner I (2006) Small scale spatial variability of organic carbon stocks in litter and solum of a forested Luvisol. *Geoderma* 136:631–642.

Singh, G., Singh, A., Singh, P., & Mishra, V. K. (2021). Chapter 4—Impact of climate change on freshwater ecosystem. In B. Thokchom, P. Qiu, P. Singh, & P. K. Iyer (Eds.), *Water Conservation in the Era of Global Climate Change* (pp. 73–98). Elsevier.

<https://doi.org/10.1016/B978-0-12-820200-5.00017-8>

Smith, J. C., Galy, A., Hovius, N., Tye, A. M., Turowski, J. M., & Schleppei, P. (2013). Runoff-driven export of particulate organic carbon from soil in temperate forested uplands. *Earth and Planetary Science Letters*, 365, 198–208. <https://doi.org/10.1016/j.epsl.2013.01.027>

Soil Survey Staff, Natural Resources Conservation Service, United States Department of Agriculture. Web Soil Survey. Available online at <https://websoilsurvey.nrcs.usda.gov/>. Accessed [02/26/2023].

Stumm, W.; Morgan, J. J. *Aquatic Chemistry: An Introduction Emphasizing Chemical Equilibria in Natural Waters*, 3rd ed.; Wiley-Interscience: New York, 1996, 1022 pp

Strawn, D. G. (2021). Sorption Mechanisms of Chemicals in Soils. *Soil Systems*, 5(1), Article 1. <https://doi.org/10.3390/soilsystems5010013>

Tank, S. E., Fellman, J. B., Hood, E., & Kritzberg, E. S. (2018). Beyond respiration: Controls on lateral carbon fluxes across the terrestrial-aquatic interface. *Limnology and Oceanography Letters*, 3(3), 76–88. <https://doi.org/10.1002/lol2.10065>

Tranvik, L., Cole, J. J., & Prairie, Y. T. (2018). The study of carbon in inland waters—from isolated ecosystems to players in the global carbon cycle. *Limnology and Oceanography Letters*, 3(3), 41–48

- Ulseth, A. J., Bertuzzo, E., Singer, G. A., Schelker, J., & Battin, T. J. (2018). Climate-Induced Changes in Spring Snowmelt Impact Ecosystem Metabolism and Carbon Fluxes in an Alpine Stream Network. *Ecosystems*, *21*(2), 373–390. <https://doi.org/10.1007/s10021-017-0155-7>
- Voss, B. M., Peucker-Ehrenbrink, B., Eglinton, T. I., Spencer, R. G. M., Bulygina, E., Galy, V., Lamborg, C. H., Ganguli, P. M., Montluçon, D. B., Marsh, S., Gillies, S. L., Fanslau, J., Epp, A., & Luymes, R. (2015). Seasonal hydrology drives rapid shifts in the flux and composition of dissolved and particulate organic carbon and major and trace ions in the Fraser River, Canada. *Biogeosciences*, *12*(19), 5597–5618. <https://doi.org/10.5194/bg-12-5597-2015>
- Wallin, M., Buffam, I., Öquist, M., Laudon, H., & Bishop, K. (2010). Temporal and spatial variability of dissolved inorganic carbon in a boreal stream network: Concentrations and downstream fluxes. *Journal of Geophysical Research: Biogeosciences*, *115*(G2). <https://doi.org/10.1029/2009JG001100>
- Ward, N. D., Bianchi, T. S., Medeiros, P. M., Seidel, M., Richey, J. E., Keil, R. G., & Sawakuchi, H. O. (2017). Where Carbon Goes When Water Flows: Carbon Cycling across the Aquatic Continuum. *Frontiers in Marine Science*, *4*. <https://www.frontiersin.org/articles/10.3389/fmars.2017.00007>
- Ward, N. D., Richey, J. E., & Keil, R. G. (2012). Temporal variation in river nutrient and dissolved lignin phenol concentrations and the impact of storm events on nutrient loading to Hood Canal, Washington, USA. *Biogeochemistry*, *111*(1), 629–645. <https://doi.org/10.1007/s10533-012-9700-9>

- Washington Department of Fish and Wildlife (1994). Estimate of Potential Summer Habitat- 60 Day Low Flow Methodology. *Appendix E in: Fish Passage Barrier Assessment and Prioritization Manual, WDFW Habitat and Lands Services Program*
- Webster, J. R., Benfield, E. F., Ehrman, T. P., Schaeffer, M. A., Tank, J. L., Hutchens, J. J., & D'Angelo, D. J. (1999). What happens to allochthonous material that falls into streams? A synthesis of new and published information from Coweeta. *Freshwater Biology*, 41(4), 687–705. <https://doi.org/10.1046/j.1365-2427.1999.00409.x>
- Wollheim, W. M., Vörösmarty, C. J., Bouwman, A. F., Green, P., Harrison, J., Linder, E., Peterson, B. J., Seitzinger, S. P., & Syvitski, J. P. (2008). Global N removal by freshwater aquatic systems using a spatially distributed, within-basin approach. *Global Biogeochemical Cycles*, 22(2).
- Wu, H., Kimball, J. S., Elsner, M. M., Mantua, N., Adler, R. F., & Stanford, J. (2012). Projected climate change impacts on the hydrology and temperature of Pacific Northwest rivers. *Water Resources Research*, 48(11). <https://doi.org/10.1029/2012WR012082>